## Author Declaration

I, the undersigned **TAHERUZZAMAN KAZI** hereby declare that I am the sole author of this thesis. To the best of my knowledge, this thesis contains no material previously published by any other person except where due acknowledgment has been made. This thesis contains no material which has been accepted as part of the requirements of any other academic degree or non-degree program, in English or any other language.

This is a true copy of the thesis, including final revisions.

Date: September, 2022
Name: TAHERUZZAMAN KAZI

Signature: _____

# Abbreviations

| | |
|---|---|
| 2D | Monolayer Culture |
| 3D | Spheroid Culture |
| ALPL | Alkaline phosphatase (Non-specific) |
| ASC | Adipose-derived stem cell |
| ASMA | Alpha smooth muscle actin |
| CAO | Combination of adipogenic and osteogenic media |
| CAO1/2 | Half diluted CAO |
| CAO1/2-FP | CAO1/2 with FGF2 and PDGF-AA |
| CTNB | β-catenin |
| DMEM | Dulbecco's modified eagle medium |
| DMEM-FBS | Dulbecco's modified eagle medium with 10% fetal bovine serum |
| DPC | Dermal papilla cell |
| DPC-EV | Extracellular vesicle derived from DPC |
| ERK | Extracellular signal-regulated kinase |
| HF | Hair follicle |
| IBMX | Isobutylmethylxanthine, 1-Methyl-3-Isobutylxanthine |
| OPN | Osteopontine |
| T-PBS | Phosphate buffered saline with Tween-20 |
| VCAN | Versican |

**Acknowledgements**

All praises are for Almighty Allah who enables me to present this dissertation for the degree of Doctor of Philosophy (PhD).

My deepest gratitude and profound appreciation to my supervisor Professor Dr. Takashi MATSUZAKI, Faculty of Life and Environmental Science, Shimane University, Shimane, Japan for giving me the opportunity to conduct my research and study under his intellectual supervision. I would thank to him for his scholastic guidance, continuous encouragement, valuable suggestions, constructive criticism, and kind help throughout the research work and in preparation of this dissertation.

I also want to express my sincere appreciation to my co-supervisor Professor Dr. Akio NISHIKAWA, Faculty of Life and Environmental Science, Shimane University, Shimane, Japan for his advice and support during the course of this research.

I am grateful to Dr. Ichitaro NIIBE, Faculty of Life and Environmental Science, Shimane University, Shimane, Japan for his kind support in research works, valuable suggestions and encouragement.

I also want to thanks my all-laboratory colleagues for their team effort, friendly behavior and enjoyable working environment.

I would like to express my sense of gratitude to the officials of Faculty of Life and Environmental Science and International Student Center, Shimane University and the United Graduate School of Agricultural Sciences, Tottori University for their kind help to facilitate my study and stay in Japan.

I deeply owe my whole hearted thanks to my current lab superior Professor Dr. Shigeki INUI. M.D. and other Lab members, Department of Regenerative Dermatology, Graduate School of medicine, Osaka University, Japan.

I express my boundless gratitude and endless thanks to my Parents and other family members for their blessing, sacrifice and patience which can never be repaid. I also thank to my relatives and friends who inspired me during the period of study in Japan.

Finally, I am grateful to my wife *Khanam Rajia* and my beloved son *Kazi Hasnat Mehran* for their assistance, patience, inspiration and care.

**TAHERUZZAMAN KAZI.**

# Table of Contents



# Chapter I

## General Introduction……..1-5

## Chapter II

## Optimal Stimulation Toward the Dermal Papilla lineage Can Be Promoted by Combined Use of Osteogenic and Adipogenic Inducers

## Chapter III

**Dermal Papilla Cell-Derived Extracellular Vesicles Increase Hair inductive gene Expression in Adipose Stem Cells via β-Catenin Activation**

## Chapter IV



# List of Figures

### Chapter II

## Chapter III



## List of Tables

# Chapter I

# General Introduction

## 1.1. Hair as an integumentary organ

Integumentary system is a set of organs which serve as barrier to protect deeper tissue and maintaining physiological function by balance water, excrete waste, thermal insulation and so on. In this system hair follicles have tremendous role in order to camouflage in many mammalians and provide ability to sense their environment specially in rodent vibrissa follicle. Unlike many mammalians, human hair follicle developed and distributed in different way, even in difference between male and female. Hair follicle especially at scalp have great importance to social and sexual communication. However, Hair loss or alopecia is the aftereffect of inefficacy in regrowing hair shafts from hair follicles (HFs) in both males and females. The HF, an integumentary organ, has a unique structure that contains numerous concentric epithelial keratinocytes and a specialized mesenchymal cell called a dermal papilla cell (DPC) [**Banka et al., 2013**]. These specialized mesenchyme derived cells are aggregated at the lower end of the HF. DPCs maintain HF development, hair cycle activity, and hair shaft growth [**Jahoda et al., 1984**]. Hormonal perturbance and extrafollicular environmental factors affect follicular stem cell properties, resulting in the loss of HFs [**Chueh et al., 2013**]. And, the most common type hair loss or alopecia named as male pattern baldness or androgenic alopecia (AGA). AGA involves continuous replacement of terminal large hair to thinner and shorter vellus [**Hamilton et al., 1951**]. To prevent hair loss, prescribed medications and hair transplantation are typical measures, but so far, they are not able to revive HFs. In addition, researchers are focusing on this tiny structure hair follicle through understanding their microenvironment and the molecular signal involved in hair follicle neogenesis.

## 1.2. **Dermal papilla cells on hair follicle organogenesis**

Mammalian hair follicles construct with specialized mesenchymal cells at the lower end of the hair bulb region known as the dermal papilla cells (DPCs), which play pivotal roles in the differentiation and proliferation of the hair matrix cells [**Miller et al., 2002**]. In the case of HF morphogenesis, DPCs intricately interact with the surrounding epithelial cells via a paracrine mechanism [**Robinson et al., 1997**]. The source cells of DPCs differentiate and

aggregate as globular structure through the sequential cross-talks with the overlaying epithelium in the developmental process of the hair follicles [**Botchkarev et al., 2003**]. These aggregates are indispensable not only for embryonic hair follicle development, but also in postnatal hair cycling [**Hardy., 1992**; **Oliver et al., 1967**]. In fact, the intact dermal papillae (DPs) can induce hair follicles de novo in the recipient skin, even if the epidermis has been derived from a non-hair-bearing region [**Inamatsu et al., 2006**]. Therefore, DPCs have been thought to possess a strong hair-forming ability; however, their nature is not clear yet.

### 1.3. The Role of ECM proteins on DPC aggregation and hair cycle

DPCs contain a large amount of the extracellular matrix (ECM) proteins such as versican (vcan) and perlecan, as well as laminin and collagen types I, III and IV [**Couchman et al.,1993, Messenger et al., 1991**]. Versican is the core protein of a multifunctional chondroitin sulfate proteoglycan [**Shinomura et al., 1993**]. Moreover, it inhibits many types of cell–substratum adhesion molecule, by which it may control cell proliferation and differentiation in organogenesis [**Yamagata et al., 1994**]. The amount of vcan in a DP increases in the anagen phase (the active growth phase of hair follicles) and reaches the maximum level; then, the expression rapidly decreases in the catagen phase (the regression phase) and is abolished by the end of the telogen phase (the resting phase) [**Westgate et al., 1991; Soma et al., 2005**]. An anagen DP is the largest compared with those in other stages, because vcan and other ECM proteins are actively secreted in anagen and deposited in the intercellular space between the DP.

### 1.4. Stimulation and of hair inductive properties in DPCs via growth factor

Once the DPs are isolated from the body and out-grown in vitro, DPCs rapidly lose their hair-forming ability upon culturing beyond five rounds of sub-cultivation [**Jahoda et al., 1984**]. Similarly, DPCs with low passage numbers express vcan at an intense level, but those with high passages tend to lose its expression [**Kishimoto et al., 1999**]. DPCs can maintain vcan expression upon continuous stimulation with appropriate growth factors, such as fibroblast growth factor 2 (FGF2) and platelet-derived growth factor (PDGF) [**Masahiro et al., 2015**]. Moreover, the hair follicle inductivity can be partially restored in a three-

dimensional (3D) culture [**Higgins et al., 2013**]. Dr. Kishimoto's team has generated vcan–GFP transgenic mice that express the GFP under the control of the vcan promoter [**Kishimoto et al. 1999**]. The GFP expression was prominent in DPCs of these mice in the anagen phase. They had clearly demonstrated the close relationship between the GFP fluorescence intensity and the hair inductivity of the DPCs that had been derived from the vcan–GFP mice. Therefore, the hair-forming activity of the DPCs can be visually monitored using the vcan–GFP mice.

### 1.5. DPC Sharing similar unique gene expression with ASC

DPCs are thought to derive from a mesenchymal lineage in the early stage of hair follicle development in embryos [**Hardy, 1992**]. Although the founder cells of DPCs are still unclear, DPCs share unique gene expression profiles with that of adipocytes and osteocytes, such as leptin and osteopontin (opn) in a hair cycle-dependent manner [**Festa et al., 2011; Tian et al., 2001]**, respectively**.** In addition, the DPCs drastically change their hair-forming ability during the different hair cycle stages. Alkaline phosphatase (alpl) is also a typical DP-specific maker gene. Alpl is expressed intensely in the dermal sheath cells covering the bottom area of the hair bulb; its expression begins in the very early stage of the anagen phase, reaches highest level in the mid-anagen phase, and rapidly ceases in the catagen phase [**Iida et al., 2007**]. Because cultured DPCs without the alpl expression lose their hair-forming ability, alpl appears to be closely related to DP-specific functions. These facts suggest that the DPCs are refreshed and recover their hair inductivity in the early anagen phase in each hair cycle, by responding to differentiation factors from the surrounding cells, some of which might be similar to the inducers of the adipogenic or osteogenic differentiation from MSCs.

### 1.6.Transdifferentiation of DPC properties into ASC via Extra cellular Vesicles (EVs)

Stem cells maintain tissue niches through self-renewal, differentiation of multi-lineage cells, and through the secretion of various types of growth factors [**Mizuno et al., 2009**]. For therapeutic options, induced-pluripotent stem cells (iPSCs), embryonic stem cells (ESCs), and adult stem cells are widely used owing to their pluripotency and auto-reproducibility, in spite of the limitations of the two former types (iPSCs and ESCs) owing to ethical

considerations and genetic manipulation [**Takahashi et al., 2006; Young et al., 2000; Lenoir et al., 2000**]. In contrast, adult stem cells have no ethical issues to be considered. Mesenchymal stem cells (MSCs) are adult stem cells that are mainly obtained from the bone marrow stroma; however, the harvesting procedure is highly invasive and the differentiation potential declines with age [**Stenderup et al., 2003**]. Adipose stem cells (ASCs), with similar cell morphology and differentiation potential as bone marrow-derived MSCs, are isolated from white adipose tissue [**Zuk et al., 2002**], which can be easily collected. White adipose tissue accumulates at various specific locations called adipocyte depots, which play definite cellular and molecular functions [**Östman et al., 1979; Lundgren et al., 2004**]. A considerable quantity of adipocyte depots is subcutaneous, while others are visceral and located in the abdominal cavity [**Schmidt et al., 2012**]. The upper layer of the subcutaneous tissue is referred to as an intradermal adipocyte depot, consisting of adipose stem-precursor cells. These cells communicate with each other via growth factors, such as platelet-derived growth factor (PDGF), during HF development and hair cycle, especially in the anagen phase of postnatal development [**Festa et al., 2011**]. In addition, ASCs can differentiate into many other cells types-that is, adipogenic and osteogenic under appropriate differentiation media. Mesenchymal stem cells (MSCs) and their descendants are known to differentiate into various cell types depending on stimulation from the cellular environment. For example, MSCs differentiate into osteocytes when they are stimulated with 100 nM dexamethasone, 10 mM b-glycerol phosphate and 50 µg/mL ascorbic acid [**Eslaminejad et al., 2013**]. Upon treatment of 3T3L1 fibroblasts with 1 µM dexamethasone, 0.5 mM Isobutylmethylxanthine (IBMX) and 10 µg/mL insulin, they differentiate into adipocytes [**Kim et al., 2009**]. Therefore, the lineage-specific development and differentiation of stem cells largely depends on the in vivo cellular microenvironment [**Peerani et al., 2007**]. To induce lineage specific differentiation of stem cells, including iPSCs, ESCs, MSCs, and ASCs, specific media mimicking the in vivo microenvironment are required [**Pawitan et al., 2014**]. Moreover, a recent study revealed that EVs released from cells play a role in cell–cell interactions as paracrine factors [**Jung et al., 2020**]. EVs carry microRNA (miRNA) and transcription factors to the nearby cell niche to regulate the functions of the cells **[Rajendra et al., 2017**]. However, the use of miRNA to induce stem cell differentiation and regulate the post-transcriptional expression of target genes has gained attention [**Narayan et al., 2016**]. In this regard, EV provides unique advantages due to carrying microRNA and protein which can

induce a specific cellular response to a target cell or recipient cell [**Yu et al.,2014**]. For instance, microRNA-1 or mir-1 and mir-449 regulate cardiomyocyte cell differentiation through targeting SOX6 (Sex determining Region Y-Box 6**) [Sluijter et al., 2010]**. Extracellular vesicle derived from Mesenchymal stem cell showed stimulation of proliferation, migration and modulation of car formation in dermal fibroblast cells **[Zhang et al., 2015]**. So, it remains unclear whether DPC derived EVs could be a key modulator of transdifferentiation of mesenchymal stem cell.

### 1.7.Objective of study

- There are several types of molecular markers that distinguish these two cell types; the typical expression markers are leptin for adipogenic cells and osteopontin for osteogenic cell. Notably, these two markers are also expressed in DPCs. Here, we examined whether the combination of adipogenic and osteogenic factors promotes DP-specific characteristics in cultured DPCs using the vcan–GFP transgenic mice and 3D culture techniques.

## Chapter II

## Optimal Stimulation Toward the Dermal Papilla lineage Can Be Promoted by Combined Use of Osteogenic and Adipogenic Inducers

### 2.1. Introduction

Mammalian hair follicles contain specialized mesenchymal cells at the proximal end of the hair bulb region known as the dermal papilla cells (DPCs), which play pivotal roles in the differentiation and proliferation of the hair matrix cells [**Miller, 2002**]. The founder cells of DPCs differentiate and aggregate through the sequential cross-talks with the overlaying epithelium in the developmental process of the hair follicles **[Botchkarev et al., 2003**]. These aggregates are indispensable not only for embryonic hair follicle development, but also in postnatal hair cycling [**Hardy,1992; Oliver,1967**]. In fact, the intact dermal papillae (DPs) can induce hair follicles *de novo* in the recipient skin, even if the epidermis has been derived from a non-hair-bearing region [**Inamatsu et al., 2006**]. Therefore, DPCs have been thought to possess a strong hair-forming ability; however, their nature is not clear yet.

DPs contain a vast amount of the extracellular matrix (ECM) proteins such as versican (*vcan*) and perlecan, as well as laminin and collagen types I, III and IV [**Couchman,1993; Messenger et al., 1991**]. *vcan* is the core protein of a multifunctional chondroitin sulfate proteoglycan [**Shinomura et al., 1993**]. It inhibits many types of cell–substratum adhesion, by which it may control cell proliferation and differentiation in organogenesis [**Yamagata et al., 1994**]. The amount of *vcan* in a DP increases in the anagen phase (the active growth phase of hair follicles) and reaches the maximum level; then, the expression rapidly decreases in the catagen phase (the regression phase) and is abolished by the end of the telogen phase (the resting phase) [**Westgate et al.,1991; Soma et al., 2005**]. An anagen DP is the largest compared with those in other stages, because *vcan* and other ECM proteins are actively secreted in anagen and deposited in the intercellular space between the DPCs.

Once the DPs are isolated from the body and outgrown in vitro, DPCs rapidly lose their hair-forming ability upon culturing beyond five rounds of sub-cultivation [**Jahoda et al., 1984**]. Similarly, DPCs with low passage numbers express vcan at an intense level, but those with high passages tend to lose its expression **[Kishimoto et al.,1991]**. DPCs can maintain vcan expression upon continuous stimulation with appropriate growth factors, such

as fibroblast growth factor 2 (FGF2) and platelet-derived growth factor (PDGF) [**Masahiro et al., 2015]**. Moreover, the hair follicle inductivity can be partially restored in a three-dimensional (3D) culture [**Higgins et al., 2013**; **Kishimoto et al.,1991]** generated vcan–GFP transgenic mice that express the GFP under the control of the vcan promoter. The GFP expression was prominent in DPCs of these mice in the anagen phase. They had clearly demonstrated the close relationship between the GFP fluorescence intensity and the hair inductivity of the DPCs that had been derived from the vcan–GFP mice **[Kishimoto et al.,1991]**. Therefore, the hair-forming activity of the DPCs can be visually monitored using the vcan–GFP mice.

DPCs are thought to derive from a mesenchymal lineage in the early stage of hair follicle development in embryos [**Hardy,1992**]. Mesenchymal stem cells (MSCs) and their descendants are known to differentiate into various cell types depending on stimulation from the cellular environment. For example, MSCs differentiate into osteocytes when they are stimulated with 100 nM dexamethasone, 10 mM β-glycerol phosphate and 50 μg/mL ascorbic acid [**Eslaminajade et al., 2013**]. Upon treatment of 3T3L1 fibroblasts with 1 μM dexamethasone, 0.5 mM Isobutylmethylxanthine (IBMX) and 10 $\mu g \cdot mL^{-1}$ insulin, they differentiate into adipocytes [**Kim et al.,2009**]. Although the founder cells of DPCs are still unclear, DPCs share unique gene expression profiles with that of adipocytes and osteocytes, such as leptin (lep) and osteopontin (opn), respectively. In addition, the DPCs drastically change their hair-forming ability during the different hair cycle stages. Alkaline phosphatase (alpl) is also a typical DP-specific maker gene. Alpl is expressed intensely in the dermal sheath cells covering the bottom area of the hair bulb; its expression begins in the very early stage of the anagen phase, reaches highest level in the mid-anagen phase, and rapidly ceases in the catagen phase [**Iida et al., 2007**]. Because cultured DPCs without the alpl expression lose their hair-forming ability, alpl appears to be closely related to DP-specific functions. These facts suggest that the DPCs are refreshed and recover their hair inductivity in the early anagen phase in each hair cycle, by responding to differentiation factors from the surrounding cells, some of which might be similar to the inducers of the adipogenic or osteogenic differentiation from MSCs. Here, we examined whether the combination of adipogenic and osteogenic factors promotes DP-specific characteristics in cultured DPCs using the vcan–GFP transgenic mice and 3D culture techniques.

## 2.2. Materials and methods

### 2.2.1. Media

Dulbecco's modified Eagle's medium (DMEM)-based adipogenic and osteogenic media were mixed at a 1:1 ratio and referred to as combination of adipogenic and osteogenic media (CAO), which contains 10% FBS, 550 nM dexamethasone (the usual working dose is 1000 nM for adipogenic and 100 nM for osteogenic; MP Biomedicals, Irvine, CA, USA), 0.5 μM IBMX (adipogenic; Fujifilm Wako Pure Chemical, Osaka, Japan), 10 μg/mL insulin (adipogenic; Sigma-Aldrich, St Louis, MO, USA), 10 mM β-glycerol phosphate (osteogenic; TCI, Tokyo, Japan) and 50 μg/mL ascorbic acid (osteogenic; Fujifilm Wako). CAO was further diluted to twice the volume with DMEM containing 10% FBS (DMEM-FBS) and referred to as half-diluted CAO (CAO1/2). In certain experiments, DMEM-FBS or CAO1/2 was supplemented with FGF2 and/or PDGF-AA (PeproTech, Rocky Hill, NJ, USA) at different concentrations.

### 2.2.2. Isolation and culture of DPCs

*vcan*–GFP mice, the *vcan* promoter-driven GFP-expressing mice, were kindly provided by J. Kishimoto (Shiseido, Japan). DPs were isolated from the vibrissa follicles, in anagen phase, of the *vcan*–GFP mice and cultured in papilla cell growth medium (Toyobo, Osaka, Japan) in an atmosphere of 5% $CO_2$ at 37°C. Outgrowing DPCs were collected by using Accutase (Innovative Cell Technologies, San Diego, CA, USA) and subculture up to passage 5 (P = 5) to propagate the cells; then, they were aliquoted and preserved in liquid $N_2$. Thawed DPCs were aliquoted and cultured in CAO, CAO1/2 or DMEM-FBS in a six-well culture plate at $6\times10^4$ cells per well. After 5 days, the cells were dissociated with Accutase and inoculated in a low-adhesive 96-well plate (Prime surface; Sumitomo Bakelite, Tokyo, Japan) at $3\times10^3$ cells per well to prepare a 3D structure known as the spheroid, for 4 or 5 days. All procedures performed in the studies involving animals were in accordance with the ethical standards of the Animal Research Committee of Shimane University, where the studies were conducted.

### 2.2.3. Measurement of spheroid characteristics

Fluorescent micrographs of each spheroid were taken every day using an inverted fluorescence microscope (Nikon Eclipse T*i*; Nikon, Tokyo, Japan). *vcan* expression in the spheroids was indicated by the GFP fluorescence intensity, and the spheroid size was estimated from the projected area of the micrographs using the IMAGEJ public domain software (NIH, Bethesda, MD, USA). Statistical analyses were performed using the *t*-test on six spheroids from each experimental group.

### 2.2.4. RNA extraction and quantitative PCR

Total RNA was obtained from the spheroids on day 4 and from the intact DPs of vibrissa follicles, as the positive control, using the RNeasy mini kit (Qiagen, Germany); cDNAs were prepared from the total RNA using the QuantiTect reverse transcription kit (Qiagen, Hilden, Germany). Quantitative PCR (qPCR) analysis was performed using the Thermal Cycler Dice® Real Time System (TP800; Takara Bio, Kusatsu, Japan) with the cDNAs and Syber Premix Ex Taq II kit (Takara Bio), to examine the gene expression levels of *vcan*, *opn*, α-smooth muscle actin and *alpl*. The expression level of the *GAPDH* gene was used as the internal control in all of the experiments.

### 2.2.5. Whole-mount immunocytochemistry

Lab-Tek II chamber slides (eight wells per slide; Thermo Fisher Scientific, Waltham, MA, USA) were coated with 30 μL/well of 0.5 mg/mL collagen I (IPC-50; Koken, Tokyo, Japan) in PBS until drying up. The spheroids of C57BL/6-derived DPCs were made as above with CAO1/2 or DMEM-FBS and transferred into the chamber slides using wide-bore pipette tips. After the spheroids attached to the surface, the culture medium was carefully removed. The spheroid was covered again with 30 μL/well of 0.5 mg/mL collagen I to prevent peeling off from the surface during immunocytochemistry. Then, the spheroids were fixed with 4% paraformaldehyde for 10 min and permeabilized with 1% Triton X-100 for 10 min at room temperature. Then, they were blocked for 30 min with Block Ace (DS Pharma Biomedical, Osaka, Japan) and treated with anti-ASMA Ig (MAB1420; R&D Systems, Minneapolis, MN, USA) or anti-ALPL Ig (AF2910; R&D Systems) at manufacturer's recommended dilution in PBS at 4 °C for overnight. They were thoroughly washed with PBS containing 0.05% Tween 20 and reacted with Alexa Flour 488- or Alexa Flour 594-conjugated secondary

antibodies at 1:800 dilution. DAPI Fluoromount G (Southern Biotech, Birmingham, AL, USA) was used for nuclei stain. Fluorescent micrographs were taken under a fluorescence microscope (BX51N; Olympus, Tokyo, Japan) aided with a digital monochrome camera (DFC345FX; Leica Microsystems, Wetzlar, Germany). The fluorescent intensities were measured for three spheroids for each category using IMAGEJ software and averaged.

### 2.2.6. Biological assay

Patch assay was carried out according to Zheng *et al.* [**Zheng et al., 2005**] with the C57BL/6-derived DPCs of passage 5. The cells were cultured in CAO1/2 supplemented with both FGF2 and PDGF-AA or DMEM-FBS for 7 days in monolayer culture. Then, $0.75 \times 10^6$ DPCs and $1.5 \times 10^6$ newborn-derived keratinocytes were mixed and inoculated into a hanging drop culture plate (Elplasia MPs500; Kuraray, Tokyo, Japan), which contains 680 micropores for making spheroids. Thus, one spheroid included ~ 1100 DPCs and 2200 keratinocytes. The spheroids were centrifuged and concentrated in 10–12 μL cell suspension and were inserted into the hypodermis of host nude mice. The patches formed underneath the skin were collected on 31 or 34 days after the transfer, embedded in OCT compound and frozen. Thin sections, 5 μm thick, were made with Leica CM 1510S cryostat and fixed with 10% neutral formalin for 10 min. The samples were stained in Mayer's hematoxylin and eosin solutions and observed under a Keyence BZ-X700 microscope (Keyence, Osaka, Japan).

## 2.3. Results.

### 2.3.1. CAO promotes the expression of DPC-related genes

We used the *vcan*–GFP mice to visually indicate the hair-inductive property of DPCs, because the expression level of *vcan* is closely related to the extent of the property. The GFP fluorescence was the strongest in anagen DPs (Fig. 1Aa), which rapidly diminished when they were cultured *in vitro* (Fig. 1A b, c). It is well known that the gene expression profiles are vastly different between the cells maintained in the two-dimensional (2D) monolayer culture and the 3D spheroid culture, and that the profile in the latter is similar to those of intact tissues. The *vcan* expression was recovered by preparing spheroids of the DPCs in the low-adhesive culture plate, but it decreased in a few days when cultured in DMEM-FBS (Fig. 1Bi–l). To enhance the activity of DPCs, we cultured the cells under a combination of

adipogenic and osteogenic factors at different concentrations (CAO or CAO1/2) for 5 days and prepared spheroids from these cells. By adding these factors, the GFP fluorescence was augmented in the spheroids of DPCs that had been cultured in CAO (CAO spheroids; Fig. 1Ba–d) or CAO1/2 (CAO1/2 spheroids; Fig. 1Be–h), compared with the control spheroids (Fig. 1Bi–l). Then, the GFP fluorescence intensity was measured for each spheroid by image analyses using the IMAGEJ software. The fluorescence was more intense in the CAO or CAO1/2 spheroids in comparison with the control on day 1, which was the day after initiating the spheroid preparation in the low-adhesive culture plate (Fig. 1C). On day 5 of the 3D culture, the GFP fluorescence in the control spheroids was reduced to 52%, but the CAO1/2 spheroids retained the fluorescence at more than 67% of the initial value (Fig. 1C). The spheroids gradually shrank during the 3D culture because the cells contacted and pulled each other, which was clearly seen as the decrease in the spheroid volume (Fig. 1B). The size reduction was more prominent in the control spheroids than in the CAO or CAO1/2 spheroids. In the intact DPs, the intercellular space is filled with a vast amount of ECM proteins, such as *vcan*. The ECM may avoid the shrinkage of the DP *in vivo*, as well as transduce the microenvironmental signals to the DPCs. qPCR revealed that the expression of *vcan* was the highest in the CAO1/2 spheroids (Fig. 2). In addition, the other two DP-related genes, ASMA (*asma*) and tissue-nonspecific *alpl*, were expressed at a higher level in the CAO1/2 spheroids (Fig. 2). Interestingly, the CAO spheroids expressed the DPC-related genes at similar levels to the control (Fig. 2), although their GFP fluorescence and size were comparable with the CAO1/2 spheroids (Fig. 1B,C). These results suggest that the CAO1/2 medium would be effective in maintaining the DPC-specific properties in the spheroids, but not enough to avoid shrinkage of the spheroids during the 3D culture.

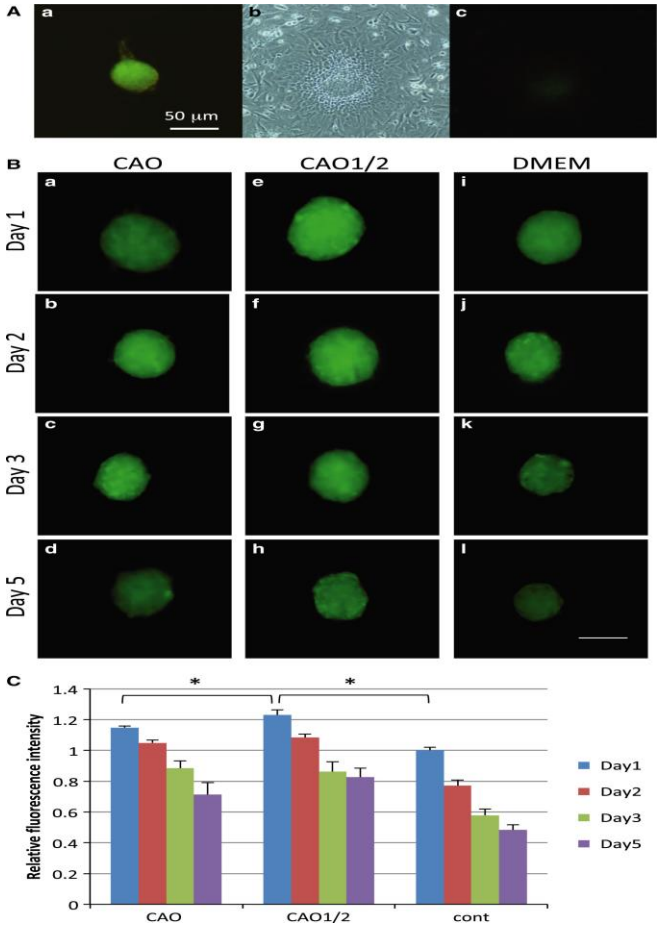


**Figure 1. *vcan* expression was stimulated in DPCs cultured with the adipogenic and osteogenic inducers.**

*vcan* expression was stimulated in DPCs cultured with the adipogenic and osteogenic inducers. DPs were isolated from the vibrissa follicles of the vcan–GFP transgenic mice in the anagen phase, which showed intense GFP fluorescence as an indication of the expression level of the *vcan* gene (Aa). The DPCs outgrown in vitro were reduced in their fluorescence (Ab, Ac). The DPCs were passaged five times in the control medium (DMEM-FBS) and were sub-cultured in the CAO (Ba-Bd), CAO1/2 (Be–h) or control (Bi–l) media for 5 days. Then, the DPCs were inoculated at $3\times10^3$cells per well in a low-adhesive 96-well plate to make a spheroid and cultured for 5 more days. The fluorescence micrographs of six spheroids from each category were taken at days 1 (Ba, Be, Bi), 2 (Bb, Bf, Bj), 3 (Bc, Bg, Bk) and 5 (Bd, Bh, Bl), from which the GFP fluorescence intensities were calculated by image analyses (C). GFP fluorescence at day 5 was strongest in the spheroids cultured in CAO1/2 and rapidly decreased in those cultured in the control medium (cont). Scale bars, 50μm (A); 100μm (B). Vertical bars indicate standard deviation (C). The difference was assessed using ANOVA with post hoc Tukey's honestly significant difference (HSD) test. Significant differences to CAO1/2 on day 1 are indicated as *P > 0.05.

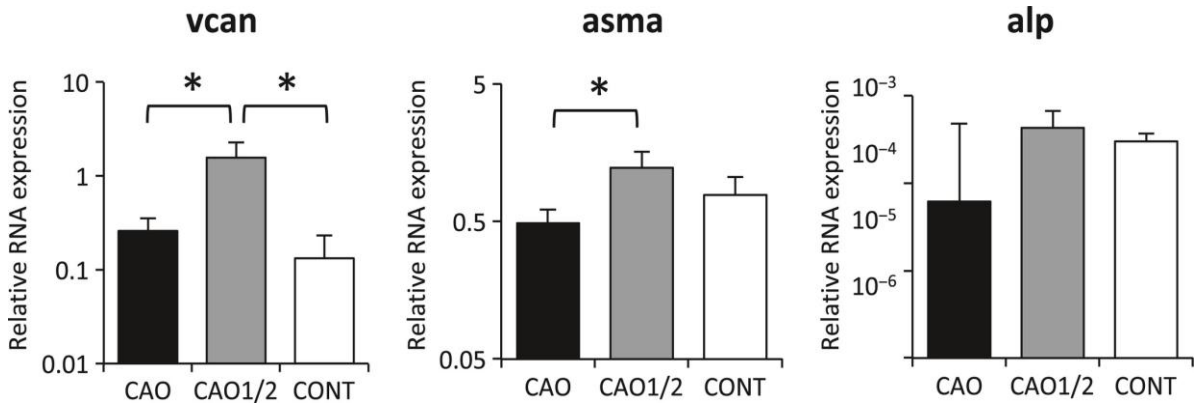


**Figure 2. Expression of DPC-related genes in the spheroids**

Total RNA was isolated from the spheroids cultured in CAO, CAO1/2 or DMEM-FBS at day 4 of the 3D culture, and cDNAs were prepared from them. The expression levels of DPC-related genes were estimated by qPCR using the cDNA and the specific primer sets for *vcan*, *asma* and *alpl*. Vertical bars indicate standard deviation. The difference was assessed using ANOVA with post hoc Tukey's HSD test. Significant differences to CAO1/2 are indicated as *P < 0.05.

### 2.3.2. FGF2 and PDGF-AA prevent spheroid shrinkage and retain vcan expression

It has been previously reported that FGF2 and PDGF-AA are positive factors for DPC proliferation *in vitro*. Thus, we examined the effect of both factors on DPC spheroids, in combination with CAO or CAO1/2. FGF2 and PDGF-AA were added at three different concentrations, namely, 20, 40 and 100 ng/mL. DPCs were cultured for 5 days and inoculated into a low-adhesive culture plate at 3000 cells per well, containing the same medium as 2D culture, to prepare the spheroids. Under the 3D condition, the control spheroids, which had been produced from DPCs cultured in DMEM-FBS, drastically shrank in 2 days (Figs 3j3, 4l and 3, 4A). Interestingly, the spheroids retained their volume and *vcan* expression when FGF2 and PDGF-AA had been added to the CAO1/2 medium (Fig. 3g–i), although these factors did not show such positive effects with CAO (data not shown). Image analyses revealed that FGF2 or PDGF-AA alone could enhance the *vcan* expression at 100 ng/mL, but not efficiently at 40 ng/mL or less, as far as judging from the GFP fluorescence (Fig. 4B); however, none of them individually could avoid the size reduction of the spheroids (Fig. 4A). In contrast, the spheroids cultured in both FGF2 and PDGF-AA, at 100 ng/mL each, did not show any shrinkage (Fig. 4A). The GFP fluorescence in these spheroids was stronger than the others, which showed a tendency to increase during cultivation for 4 days without medium change (Fig. 4B). Adding FGF2 and PDGF-AA at 100 ng/mL each into the control DMEM-FBS also increases the volume of the spheroids and the GFP fluorescence, but such stimulating effects rapidly diminished within 3 days (Fig. 4). These results suggest that the combination of FGF2 and PDGF-AA at higher concentrations would promote a vast amount of ECM molecules such as *vcan*, which supports the construction and maintenance of the cohesive and flexible 3D structure of the DP.

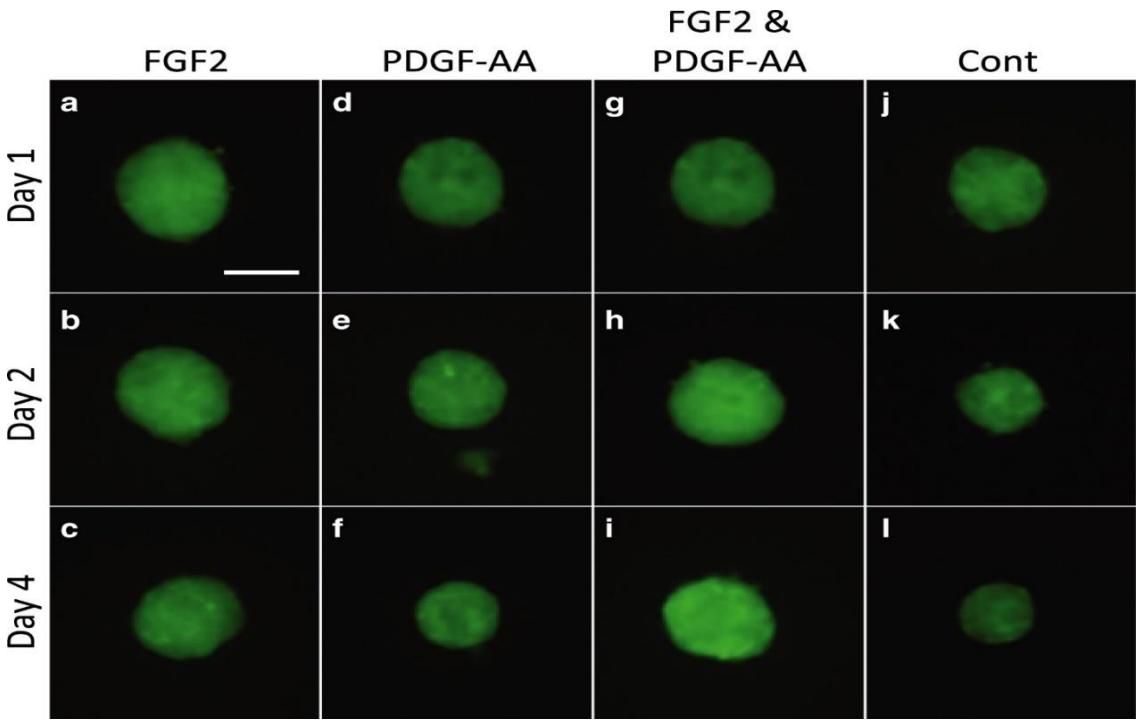


**Figure 3. FGF2 and PDGF-AA prevented the shrinkage of DPC spheroids.**

Spheroids of the vcan–GFP mouse-derived DPCs shrank during the 3D culture for 4 days in the control medium DMEM-FBS (j–l). The shrinkage was prevented by the addition of FGF2 in CAO1/2 (a–c, g–i), but not by addition of PDGF-AA alone (d–f). Interestingly, GFP fluorescence was augmented in the spheroids cultured in CAO1/2 supplemented with both FGF2 and PDGF-AA compared with in those stimulated with one of these factors alone. Scale bar, 100 μm

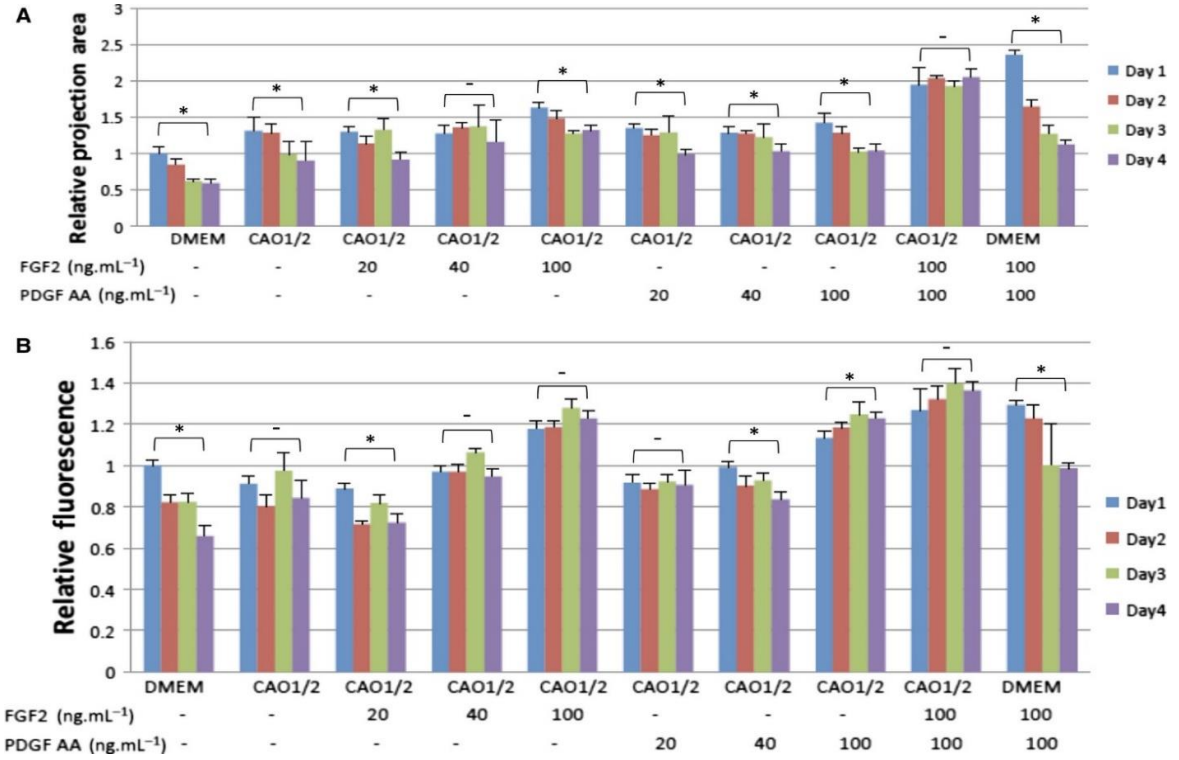


**Figure 4. vcan expression and the volume of the DPC spheroids were promoted by the addition of FGF2 and PDGF-AA during the 3D culturing.**

DPCs spheroids were cultured in the CAO1/2 or control DMEM-FBS, with or without FGF2 and PDGF-AA at 20, 40 or 100 μg/mL. The size of the spheroids was analyzed from fluorescence micrographs (A). The size is indicated as its projection area. The average size of three spheroids was the largest in those stimulated with both FGF2 and PDGF-AA in CAO1/2, which could be retained at its initial value for at least 4 days. In contrast, the spheroids cultured in DMEM-FBS shrank drastically. The vcan expression was estimated from the GFP intensity by image analyses (B). The vcan expression was promoted in the DPC spheroids by stimulation with FGF2 or PDGF-AA in a dose-dependent manner. The factors showed a synergistic effect on the upregulation of vcan gene expression and could maintain the expression level for at least 4 days. The vcan expression was also stimulated in the spheroids cultured in DMEM-FBS with FGF2 and PDGF-AA, but it dropped within 3 days in the 3D culture. Vertical bars indicate standard deviation. Statistical analyses were performed using the t-test between days 1 and 4 in each experimental group. The difference was assessed using ANOVA with post hoc Tukey's HSD test. Significant differences are indicated as *$P < 0.05$.

### 2.3.3. Synergistic effects of FGF2 and PDGF-AA with CAO1/2 medium on the expression of DP related gene

Next, we examined the effects of FGF2 and PDGF-AA on the expression of DPC-related genes in the DPC spheroids. The DPC spheroids cultured in DMEM-FBS expressed the *vcan* gene vigorously when they were stimulated with both FGF2 and PDGF-AA at 100 ng/mL (DMEM-FP spheroids; Fig. 5A). Although the average *vcan* expression was very high in the spheroids cultured in CAO1/2 medium even without FGF2 and PDGF-AA stimuli, it could be further promoted by FGF2 and PDGF-AA (Fig. 5A). FGF2 and PDGF-AA intensely augmented the expression of the *alpl* gene in the spheroids regardless of the type of media (Fig. 5B). The *alpl* expression in the CAO1/2-FP spheroids were ~ 10-fold more than that in the DMEM-FP spheroids and 200-fold more than that in the DMEM spheroids. FGF2 and PDGF-AA intensely induced the *asma* gene expression in the spheroids cultured in DMEM-FBS, but they did not show additional effects in those cultured in the CAO1/2 medium, which could vigorously increase the gene expression in comparison with the DMEM spheroids (Fig. 5C). The expression of an osteocyte marker gene, *opn*, was also stimulated more than 5-fold in the DPC spheroids that were treated with FGF2 and PDGF-AA compared with those without the stimuli, but no difference was observed between the DMEM-FP spheroids and CAO1/2-FP spheroids (Fig. 5D). These results suggest that the synergistic effect of these factors and CAO1/2 medium is obvious on *vcan* and *alpl* expressions. As suggested by the GFP fluorescence shown in Fig. 3, the average *vcan* expression in the CAO1/2-FP spheroids was higher than that in the spheroids treated with one of the factors, although a significant difference was not detected between the spheroids cultured in CAO1/2 with PDGF-AA and the CAO1/2-FP spheroids (Fig. 6A). The expression of the *alpl* gene was also stimulated in the CAO1/2-FP spheroids to a level similar to that in the intact DPs (Fig. 6B). Similarly, FGF2 and PDGF-AA showed synergistic effects on the *asma* expression in the spheroids cultured in the CAO1/2 medium (Fig. 6C). The expression of the *opn* gene was also enhanced in the CAO1/2-FP spheroids to a comparable level with that in the intact DPs (Fig. 6D). Thus, both FGF2 and PDGF-AA would be indispensable to promote DP-specific characteristics under the 3D culture condition.

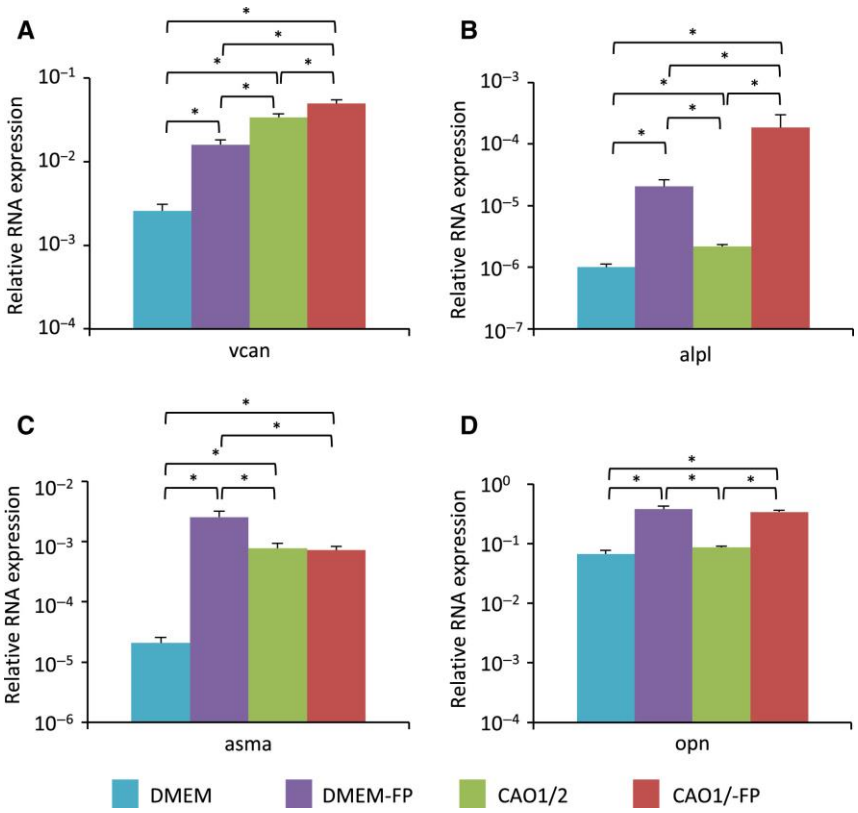


**Figure 5. Expression levels of the DPC-related genes in the DPC spheroids**

Spheroids were prepared in CAO1/2 medium or in the control DMEM-FBS, with or without FGF2 and PDGF-AA. The total RNAs were extracted from the spheroids on day 4 of the 3D culture and converted to cDNAs, which were used for qPCR analyses with specific primer sets for the DPC-related genes, *vcan*(A), *alpl*(B), *asma* (C) and *opn*(D). The average gene expression for each category was obtained from two independent experiments with triplicate measurements and shown with the standard deviation. The difference was assessed using ANOVA with post hoc Tukey's HSD test. Significant differences are indicated as *P < 0.05.

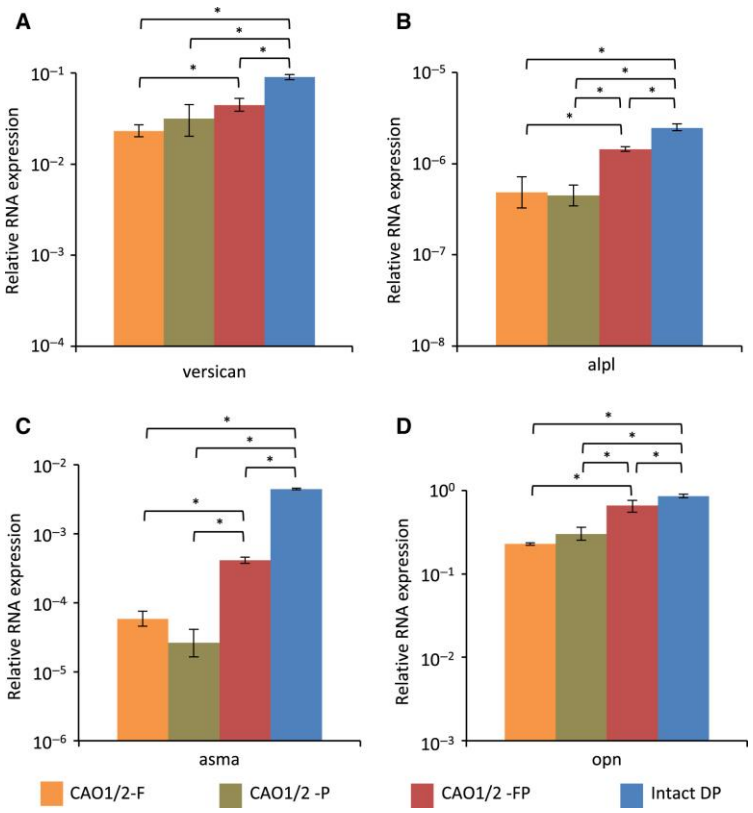


**Figure 6. Comparison of the expression of the DPC-related genes in DPC spheroids with that in intact papillae**

Total RNA was extracted from the spheroids cultured under various conditions and from the intact DPs isolated from the vibrissa follicles. The total RNA was reverse transcribed and used in qPCR analyses of the DP-related genes *vcan*(A), *alpl*(B), *asma*(C) and *opn*(D). The average gene expression for each category was obtained from two independent experiments with triplicate measurements and shown with the standard deviation. The difference was assessed using ANOVA with post hoc Tukey's HSD test. Significant differences are indicated as *P < 0.05.

### 2.3.4. CAO1/2-FP promoted ASMA and ALPL protein expression and stimulated the hair-forming activity of DPC spheroids

We compared the expression levels of ASMA and ALPL protein among CAO1/2, CAO1/2-F, CAO1/2-P and CAO1/2-FP spheroids by whole-mount immunocytochemistry with fluorescent dye-conjugated antibodies on days 1 and 4 of the 3D culture (Figs 7 and 8). Immunofluorescence of ASMA was the strongest in the CAO1/2-FP spheroids on day 1 (Fig. 7d), and the expression lasted for at least 4 days (Fig. 7i). The other spheroids showed only a weak fluorescence. The control spheroids made of DPCs cultured in DMEM-FBS tended to collapse, and most cells were dispersed during immunocytochemistry (Fig.**7**e). The expression of ASMA protein in the CAO1/2-FP spheroids was 4-fold higher than that in the CAO1/2 spheroids on average on day 4 (Fig. 9A). The ALPL expression in the spheroids was similar to those of ASMA (Fig.8). The CAO1/2-FP spheroids showed intense immunofluorescence for ALPL (Fig. 8d,h), which was 6-fold stronger than that of the CAO1/2 spheroids on day 4 (Fig. 9B). In addition to the strong expression of ASMA and ALPL, the CAO1/2-FP spheroids sustained their globular and cohesive structure, whereas other spheroids tended to be loosened or dissociated in 4 days. Although FGF2 or PDGF-AA alone could promote the expression of ASMA and ALPL protein (Fig. 9), the synergistic effects of the factors were clearly shown on expression of DPC-related proteins and also sustaining the spheroid structure and function. Finally, the hair-forming activity of the spheroids was examined using a patch assay. Mixed spheroids were prepared from keratinocytes and DPCs cultured in CAO1/2-FP or DMEM-FBS and transplanted in the hypodermis of nude mice. Epithelial cysts were observed after 31 or 34 days of the spheroid transfer (Fig. 10A, B). Hair shafts were observed in two out of three patches induced with the CAO1/2-FP spheroids, but no hair was found in the patches formed with the DMEM spheroids. Typical hair follicle structures with a hair bulb were formed in the epithelial cysts derived from the CAO1/2-FP spheroids (Fig. 10C), but only hair follicle-like structures without hair shafts were detected in histological sections of the patches formed from the DMEM spheroids (Fig. 10D). Although the produced hair shafts were small in number, there was a clear contrast between the CAO1/2-FP spheroids and the DMEM spheroids on the hair-forming ability (Table 1). These results suggest that DPCs are able to recover their hair-forming activity by culturing in CAO1/2 medium supplemented with FGF2 and PDGF-AA.

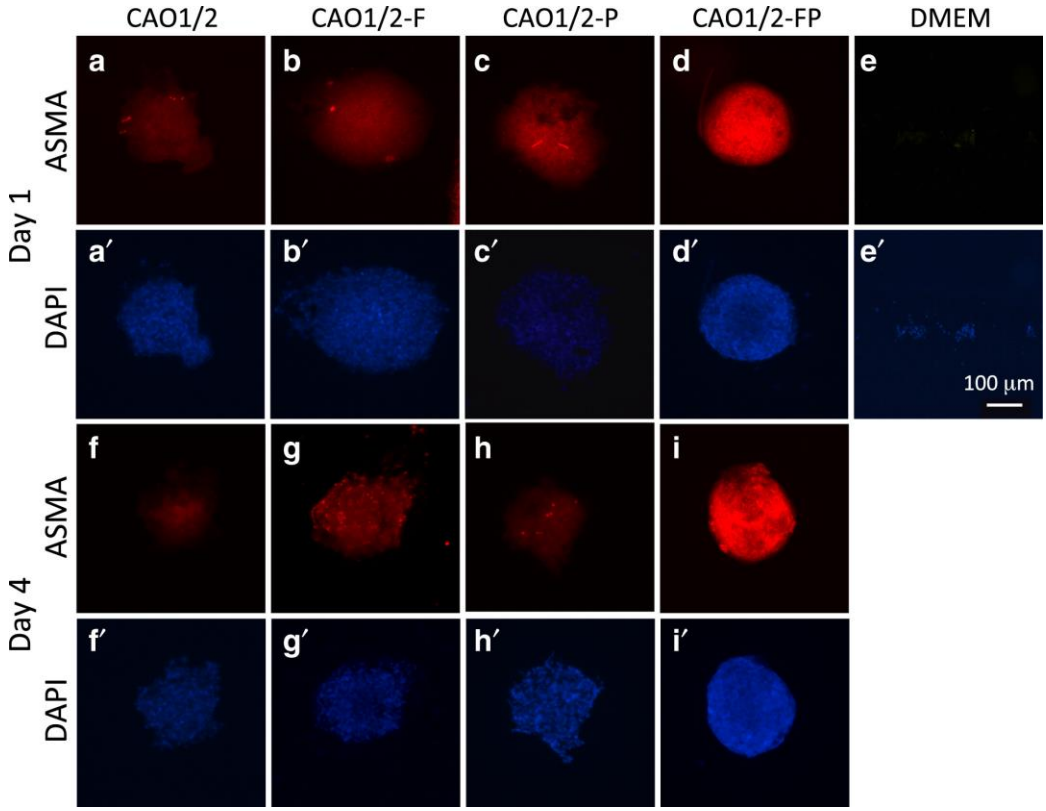


**Figure 7. The effects of FGF2 and PDGF-AA on ASMA expression in the DPC spheroids.**

The expression of ASMA protein was detected in the spheroids of the DPCs on days 1 (a–e) and 4 (f–i) of 3D culture by immunocytochemistry using anti-ASMA Ig and Alexa Fluor 594-conjugated secondary antibody. Nuclei were counterstained with DAPI (a′–i′). The fluorescence was weaker in the spheroids cultured with CAO1/2 only (a, f), CAO1/2-F (b, g) or CAO1/2-P (c, h) compared with that with CAO1/2-FP (d, i). The spheroids of the DPCs cultured with DMEM-FBS were used as negative control, which showed a tendency to disperse during the antibody treatment (e). Scale bar, 100 μm.

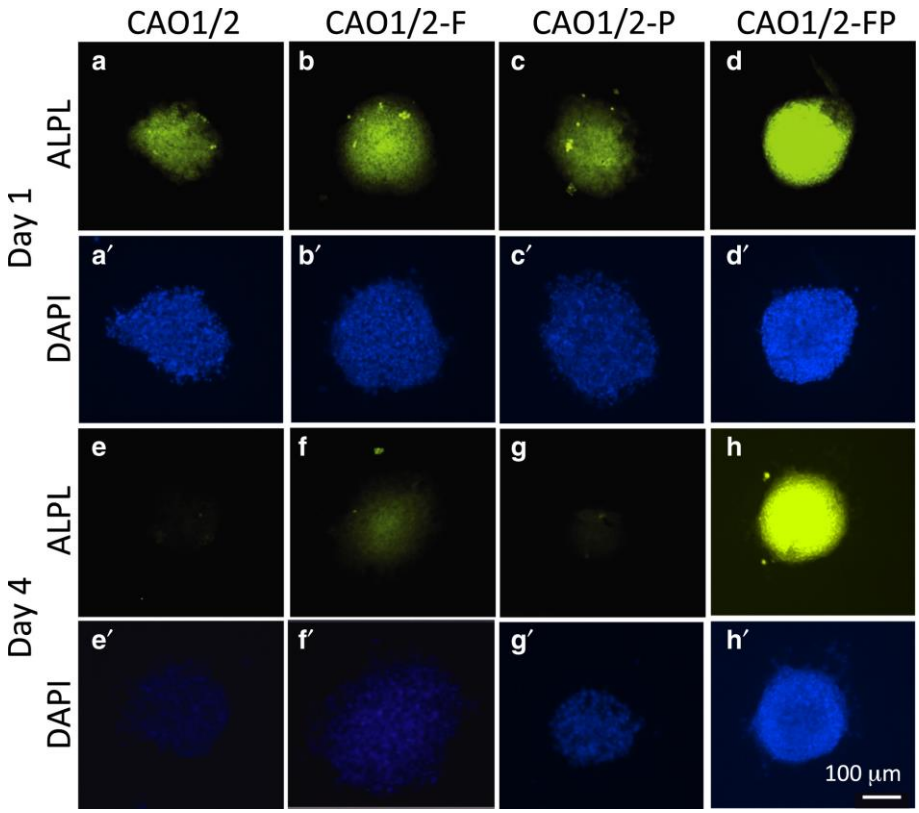


**Figure 8. The effects of FGF2 and PDGF-AA on ALPL expression in the DPC spheroids**

The expression of ALPL protein was detected in the spheroids of the DPCs on days 1 (a–d) and 4 (e–h) of 3D culture by immunocytochemistry using anti-ALPL Ig and Alexa Fluor 488-conjugated secondary antibody. Nuclei were counterstained with DAPI (a′–h′). Similar to ASMA, the DPC spheroid cultured with CAO1/2-FP (d) showed higher ALPL expression than those with CAO1/2 (a), CAO1/2-F (b) or CAO1/2-P (c). The expression of ALPL lasted for 4 days in the spheroids with CAO1/2-FP (h) but quickly decreased in those with CAO1/2 (e), CAO1/2-FGF2 (f) and CAO1/2-PDGF-AA (g). Scale bar, 100 μm

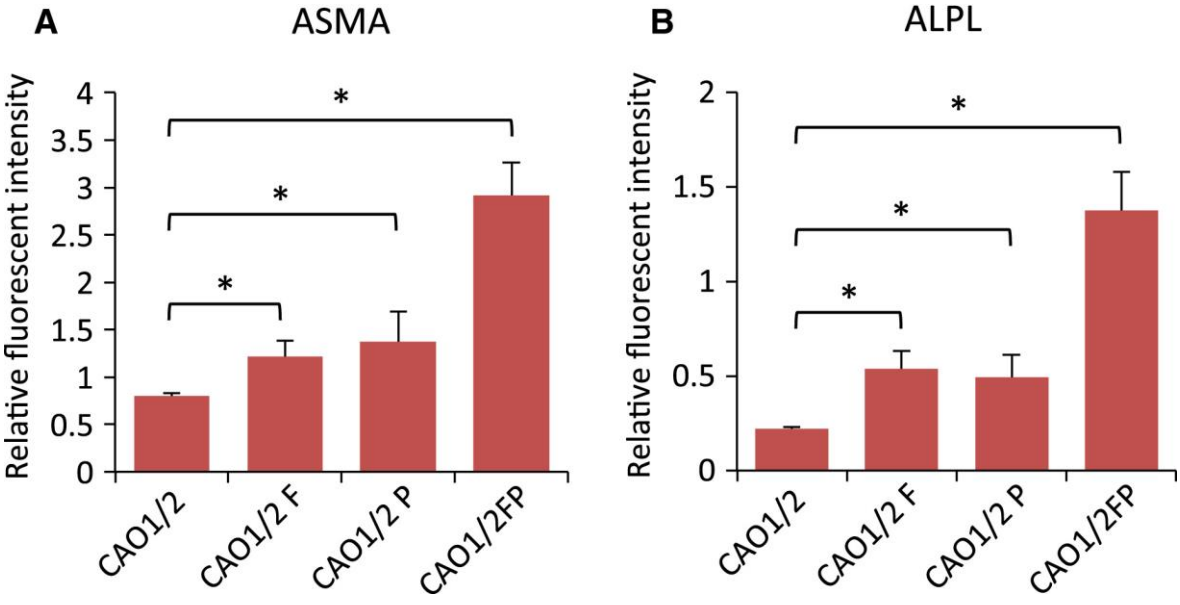


**Figure 9: FGF2 and PDGF-AA synergistically augment the expression of ASMA and ALPL in DPC spheroids.**

DPCs were cultured with CAO1/2 with or without FGF2 (F) or PDGF-AA (P) and 3D cultured for 4 days. The protein expressions of ASMA and ALPL were visualized by whole-mount immunocytochemistry with fluorescent dye-conjugated antibodies as shown in Figs 7 and 8. The expression levels of ASMA (A) and ALPL (B) were estimated from the fluorescent intensities using ImageJ software. Vertical bars indicate standard deviation. The difference was assessed using ANOVA with post hoc Tukey's HSD test. Significant differences to CAO1/2 are indicated as *P > 0.05.

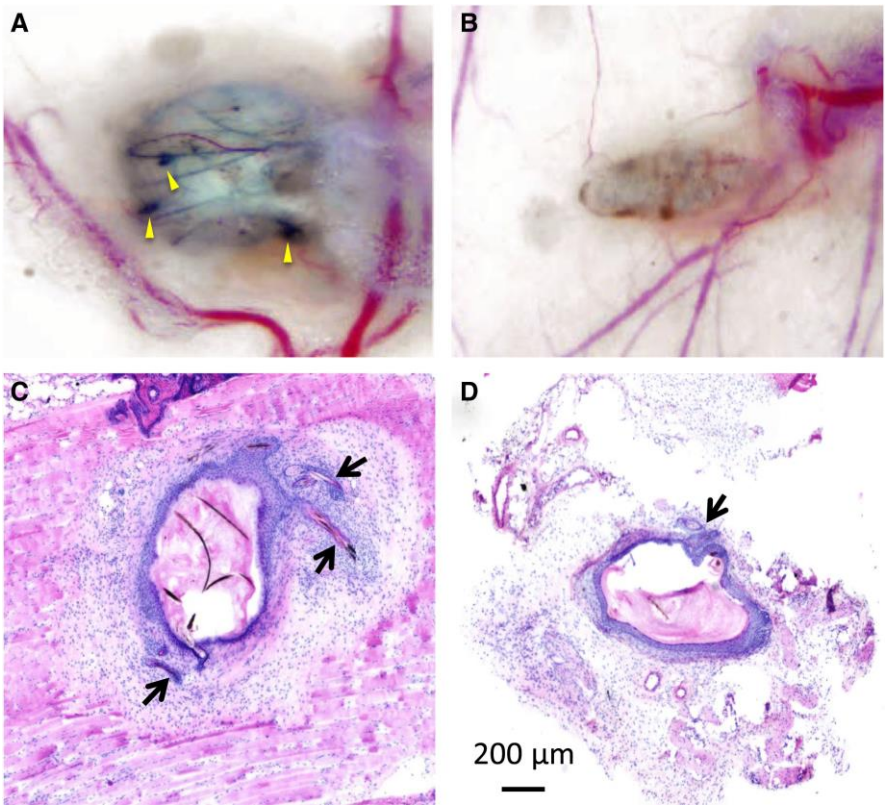


**Figure 10. Spheroids of DPCs cultured with CAO1/2-FP recovered the hair-forming ability**.

Spheroids were made from DPCs cultured with CAO1/2-FP or DMEM-FBS and newborn-derived keratinocytes, which were inserted into the hypodermis of host nude mice for a patch assay. Hair shafts were produced in an epithelial cyst formed with CAO1/2-FP spheroids (A), but not with DMEM spheroids (B). Yellow arrowheads point to the hair bulbs. In the hematoxylin and eosin-stained histological sections, typical hair follicles were detected in association with the cyst formed with CAO1/2-FP spheroids (C). Hair follicle-like structures were found in the cyst formed with DMEM spheroids in one out of three patches, but no hair bulb or shaft was observed (D). Arrows indicate hair follicle-like structures. Scale bar, 200 μm.

## 2.4. Discussion

One of the ultimate challenges of DPC culture is to generate hair follicles *de novo* by transplanting them in the sites of hair loss; however, the hair-inductive capacity of DPCs is perturbed during 2D monolayer culturing. Preparation of spheroids of DPCs is a solution for hair regeneration because the cells retain their original hair-forming properties in the 3D structure formed, with appropriate ECM molecules including *vcan*. In fact, the dispersal of aggregation in DPs leads to interference in the hair follicle formation in the developmental process [**Jacobson,1996**]. Moreover, loss of cell–cell adhesion *in vivo* appears to initiate the DP miniaturization and androgenic alopecia [J**ahoda, 1998]**. However, it is still difficult to maintain the cellular viability and also the hair-forming capacity of DPC spheroids *in vitro* because of the rapid shrinkage of the spheroids during the 3D culturing. The shrinkage would cause cell death of the DPCs in the central oxygen-poor area and disturbance in the cell–cell or cell–ECM interactions.

To overcome these problems, we had hypothesized that DPC spheroids can self-organize their structure and functions even *in vitro* by producing appropriate species and amounts of ECM proteins, if the DPC-specific differentiation is promoted. We have identified a better condition to maintain the properties of the DPC spheroids, in which the cells were stimulated with both the adipogenic and osteogenic factors, at a concentration lower than those used for inducing adipocytes or osteocytes from MSCs. This hypothesis was based on the observation that DPCs express the marker genes of both adipocytes and osteocytes. The CAO is a mixture of the adipogenic medium and the osteogenic medium, and the CAO1/2 contains the factors diluted to half of that in CAO. Because CAO1/2 was better than CAO for DPC-related gene expression (Fig. 2), it appears that the differentiation toward DPC lineage requires a relatively weaker level of stimulation than the optimal levels for the adipogenic or osteogenic lineage. In fact, the cells cultured in CAO1/2 have neither Oil Red O-positive lipid droplets nor Alizarin Red S-positive calcium deposition, which are typical characteristics for adipocytes and osteocytes, respectively. CAO1/2 contains both the osteogenic and adipogenic factor dexamethasone; two osteogenic inducers, β-glycerol phosphate and ascorbic acid; and two adipogenic additives, IBMX and insulin. In addition, CAO1/2 supplemented with FGF2 and PDGF-AA avoided the spheroid shrinkage (Figs 3 and 4) and enhanced the expression of the DPC-related genes (Figs 5 and 6) and proteins (Figs 7-9).

Thus, the combination of these factors at appropriate doses would be critical to exert and maintain the DPC-specific properties.

Although the exact roles of the factors used in this study are not yet uncovered, dexamethasone induces Runx2 expression by FHL2/β-catenin-mediated transcriptional activation. The enhanced Runx2 activity leads the adipose-derived stem cells to secrete collagen type I [**Langenbach et al.,2013]**. β-Glycerol phosphate provides phosphate to produce hydroxyapatite in the osteocyte precursor cells and also influences intracellular signaling molecules [**Langenbach et al.,2013**]. IBMX is a nonselective phosphodiesterase inhibitor and raises intracellular cAMP and protein kinase A, which activates the transcription factor peroxisome proliferator-activated receptor γ (PPARγ) required for adipogenic gene expression [**Kim et al., 2010**]. Insulin stimulates deoxyglucose uptake and glycolysis. Because the targeted deletion of PPARγ in follicular stem cells in mice causes a scarring alopecia-like phenotype [**Kim et al., 2010**], IBMX-mediated PPARγ expression may support the gene expression required for hair formation. Ascorbic acid appears to enhance the stemness of adipose-derived stem cells by stimulating collagen synthesis through the extracellular signal-regulated kinase 1/2 pathway. The adipose-derived stem cells treated with ascorbic acid promote differentiation toward endothelial and epidermal lineages in the cutaneous wound tissue [**Yu et al., 2014**].

DPCs change their gene expression profile during the hair cycle, which is closely related to the transition of DP between the active and quiescent modes. For example, *alpl* expression is stronger in the early anagen DP, gradually decreases from the bottom of the DP in the mid-anagen phase, and rapidly diminishes in the catagen phase [**Iida et al., 2007**]. Some DPCs and dermal sheath cells also express *sox-2*, which is expressed in various precursor cells, such as the MSCs. These facts suggest that the DP is composed of heterogeneous cells, and the property of each DPC may greatly change during the hair cycle depending on the microenvironment, which partially explains why we could restore the DPC-specific properties in the 3D culture by stimulation with FGF2 and PDGF-AA, in addition to the adipogenic and osteogenic factors. FGF2 increased the volume of the spheroids in a dose-dependent manner, but PDGF-AA was not effective on the volume enlargement, at least not in a range from 20 to 100 ng/mL (Fig. 4A). Because the inoculated cell number was the same as that in the spheroids, the difference in the spheroid volume would mainly be due to the

difference in the amount of the ECM molecules in the spheroids. In addition, GFP fluorescence, which is a good indication of *vcan* expression level, also increased upon stimulation with FGF2 in a dose-dependent manner (Fig. **4**B). Interestingly, PDGF-AA could synergistically act with FGF2 and increase the spheroid volume to more than that when stimulated with FGF2 only, although PDGF-AA alone did not show any effect on spheroid enlargement as mentioned above. Thus, one of the roles of FGF2 should be to stimulate ECM molecule production including *vcan*, which is important for providing hair-inductive property to the DPCs. It is known in a study of idiopathic pulmonary fibrosis that both FGF and PDGF-AA receptors cooperatively promote differentiation of fibroblasts into myofibroblasts, which leads to excessive deposition of ECM proteins in the interstitial space [**Wollin et al., 2015**]. Dermal sheath cells are closely related to myofibroblasts because both cell types vigorously express the *asma* gene. They are thought to be reservoirs of DPCs that may be partially replaced in early anagen phase to recover their hair-inducing activity and to change hair thickness [**Jahoda et al., 2001**]. Thus, FGF and PDGF-AA may also support DPC properties through the expression of the myofibroblast-related genes including *asma*.

DPCs share the expression of characteristic genes in other cell types, such as *leptin* in adipocytes and *opn* in osteocytes. It is not surprising because DPCs, as well as adipocytes and osteocytes, are thought to be derived from similar precursors. Iguchi *et al*. [**Iguchi et al., 2001**] reported that human DPCs produced leptin, but a monolayer culture of DPCs in adipogenic medium did not induce any lipid vacuoles, suggesting that unknown autocrine factors of DPCs may inhibit their differentiation toward the adipocyte lineage [**Iguchi et al., 2001**]. *opn* is expressed in MSCs cultured in the osteogenic medium, which has a versatile role in the cell–ECM interaction and anti-inflammation in osteoblasts and osteoclasts. Although the function of *opn* is less clear in DPCs, its expression is found at a certain level in DPs during the entire hair cycle and increases in shrunk DPs of catagen hair follicles, which may promote the formation of a tightly aggregated DP and protect the DPCs from apoptosis that might be induced by cytokines or hypoxia during the catagen phase [**Yu et al., 2001**].

It has been previously reported that FGF2 has mitotic activity on dermal fibroblasts in vitro [**Burgess et al., 1989**] and stimulates the cell proliferation of DPCs

derived from sheep hair follicles [**Pisansarakit et al., 1991**], although proliferation seldom occurs in DPCs in vivo. PDGF-AA is one of the key molecules secreted from adipose precursor cells in the dermis as a paracrine factor, which promotes hair follicle development and hair growth [**Festa et al., 2011**]. We cultured DPCs with FGF2 and PDGF-AA in CAO1/2 medium as a monolayer culture for only 3–4 days before preparing the spheroids, because long-term cultivation might induce apoptosis and reduce ALPL activity [**Ohyama et al., 2012**]. CAO1/2-FP spheroids could be maintained without shrinkage for 4 days (Figs 3 and 4A) and express vcan, asma, alpl and opn genes to levels nearly comparable with those in the intact DPCs (Figs 5 and 6). Furthermore, the CAO1/2-FP spheroids synthesized ASMA and ALPL proteins at a higher level (Figs 7-9) and could recover their hair-forming activity (Fig. 10). The DPCs in the DMEM spheroids showed a tendency to dissociate during the immunocytochemical treatment, which suggests that CAO1/2-FP could strengthen the cellular cohesion in the spheroids. Although a part of these effects should be explained by enrichment of ECM proteins, other molecules induced by the factors would be required to exert the full function of the active DP. In this study, we have found the way to promote and sustain the DPC-specific property in vitro, which allows us to compare comprehensively the DPCs that lost the hair-forming activity and those that recovered the activity in the future.

## 2.5. Conclusion

CAO1/2 medium consisting of adipogenic and osteogenic inducers can promote the expression of vcan in DPC spheroids, which is closely related to the hair-inductive property, and this medium when supplemented with FGF2 and PDGF-AA was able to prevent spheroid shrinkage, in addition to stimulation of the expression of DPC-related genes and recovery of the hair-forming activity. These facts indicate that adipogenic and osteogenic factors, combined with FGF and PDGF-AA, would induce the self-organization of DPCs in 3D culture, to make the structure and functions similar to that in intact DPs, by sustaining appropriate cell–cell and cell–ECM interactions to exert the hair-forming activity.

**Table I**

| Culture medium | Specimen number | Number of hair shafts |
|---|---|---|
| CAO1/2-FP | 1 | 18 |
| | 2 | 0 |
| | 3 | 8 |
| DMEM | 1 | 0 |
| | 2 | 0 |
| | 3 | 0 |

Number of hairs produced in the cysts in the hypodermis of host nude mice that had been transplanted with the cell mixture of keratinocytes and DPC spheroids cultured with CAO1/2-FP or DMEM-FBS.

## Chapter III

## Dermal Papilla Cell-Derived Extracellular Vesicles Increase Hair Inductive Gene Expression in Adipose Stem Cells via β-Catenin Activation

### 3.1. Introduction

Hair loss or alopecia is the aftereffect of inefficacy in regrowing hair shafts from hair follicles (HFs) in both males and females. Hormonal perturbance and extrafollicular environmental factors affect follicular stem cell properties, resulting in the loss of HFs [**Chueh et al., 2013**]. To prevent hair loss, prescribed medications and hair transplantation are typical measures, but so far they are not able to revive HFs. The HF, an integumentary organ, has a unique structure that contains numerous concentric epithelial keratinocytes and a specialized mesenchymal cell called a dermal papilla cell (DPC) [**Banka et al., 2013**]. These specialized mesenchyme-derived cells are aggregated at the lower end of the HF. DPCs maintain HF development, hair cycle activity, and hair shaft growth [**Jahoda et al., 1984; Jahoda et al., 1984**]. In the case of HF morphogenesis, DPCs intricately interact with the surrounding epithelial cells via a paracrine mechanism [**Robinson et al., 1997**]. A recent study revealed that EVs released from cells play a role in cell–cell interactions as paracrine factors [**Jung et al., 2020**]. EVs carry microRNA (miRNA) and transcription factors to the nearby cell niche to regulate the functions of the cells [**Rajendran et al., 2017**]. In recent years, the use of miRNA to induce stem cell differentiation and regulate the post-transcriptional expression of target genes has gained attention [**Narayanan et al.,2016**].

Stem cells maintain tissue niches through self-renewal, differentiation of multi-lineage cells, and through the secretion of various types of growth factors [**Mizuno 2009**]. For therapeutic options, induced-pluripotent stem cells (iPSCs), embryonic stem cells (ESCs), and adult stem cells are widely used owing to their pluripotency and auto-reproducibility, in spite of the limitations of the two former types (iPSCs and ESCs) owing to ethical considerations and genetic manipulation [**Takahashi et al., 2006; Young 2000; Lenoir et al., 2000**]. In contrast, adult stem cells have no ethical issues to be considered. Mesenchymal stem cells (MSCs) are adult stem cells that are mainly obtained from the bone marrow stroma; however, the harvesting procedure is highly invasive and the differentiation potential declines with age [**Stenderup et al., 2003**]. Adipose stem cells (ASCs), with similar cell morphology and differentiation potential as bone marrow-derived MSCs, are isolated from white adipose

tissue [**Zuk et al.,2002**], which can be easily collected. White adipose tissue accumulates at various specific locations called adipocyte depots, which play definite cellular and molecular functions [**Ostman et al.,1979; Lundgren et al.,2004**]. A considerable quantity of adipocyte depots is subcutaneous, while others are visceral and located in the abdominal cavity [**Schmidt et al., 2012**]. The upper layer of the subcutaneous tissue is referred to as an intradermal adipocyte depot, consisting of adipose stem/precursor cells. These cells communicate with each other via growth factors, such as platelet-derived growth factor (PDGF), during HF development and hair cycle, especially in the anagen phase of postnatal development [**Festa et al., 2011**]. In addition, ASCs can differentiate into many other cell types—that is, adipogenic and osteogenic—under appropriate differentiation media. There are several types of molecular markers that distinguish these two cell types; the typical expression markers are leptin for adipogenic cells and osteopontine for osteogenic cell. Notably, these two markers are also expressed in DPCs, in a hair cycle-dependent manner.

DPCs are derived from mesenchymal cells, and both DPCs and mesenchymal stem cells have a similar hair induction-related gene expression, such as the leptin (Lep) and osteopontin genes [**Festa et al., 2011**; **Tian et al., 2001**]. The lineage-specific development and differentiation of stem cells largely depends on the in vivo cellular microenvironment [**Peerani et al., 2007**]. To induce lineage-specific differentiation of stem cells, including iPSCs, ESCs, MSCs, and ASCs, specific media mimicking the in vivo microenvironment are required [**Pawitan, 2014**]. The aim of the study was to characterize DPC-EVs and examine the possible role of DPC-EVs in the differentiation of ASCs into DPC-like cells. This was achieved by analyzing miRNA expression in combination with a specialized medium to imitate the DPC microenvironment.

### 3.2. Materials and method

#### 3.2.1. EV Depleted FBS and EV Isolation

To avoid contamination, FBS was filtered with a 0.22 μm filter (Merck, Burlington, MA, USA), followed by ultracentrifugation at 120,000× *g* for 18 h in a fixed-angle rotor 70ti (Beckman Optima L-90K, Beckman Coulter, Brea, CA, USA). FBS-derived EVs were pelleted at the bottom of the tube, and the supernatant was collected as EV-depleted FBS. For EVs isolation from the culture medium, B6-DPCs were cultured in a 100 mm dish up to

70–80% confluence. The cells were washed three times with phosphate-buffered saline (PBS) and then cultured in DMEM-FBS (EV-depleted) for 48 h. Serial centrifugations were conducted at 4 °C from cell pellet removal to EV purification. First, a 10 min 300× *g* centrifugation was used to eliminate the cell pellet, then centrifugation at 2000× *g* for 20 min was employed to eliminate the dead cells. To eliminate cell debris and large particles, centrifugation was performed at 10,000× *g* for 30 min. Thereafter, the supernatant was collected and non-gradient ultracentrifugation was performed at 100,000× *g* for 70 min. For EV purification and elimination of protein contamination, supernatant was gently removed. The pellet was resuspended in cold PBS, and ultracentrifugation at 100,000× *g* was performed for 70 min. After resuspension, the EVs were preserved at −80 °C.

### 3.2.2. Immuno-Electron Microscope (IEM)

IEM analysis was used to confirm the presence of DPC-EVs in the conditioned medium. For fixation, equal volumes of EVs and 4% paraformaldehyde were absorbed by formvar carbon-coated EM grids for 30 min and washed twice with PBS for 3 min. The grid was rinsed 4 times with 50 mM glycine in PBS for 3 min, then blocked with Blok-Ace for 30 min and incubated with anti-CD63 for 1 h at 1:100 ratio. The antibody was washed with PBS and 0.05% Tween-20 (T-PBS) for 3 min and treated with 10 nm gold particles conjugated with a secondary antibody for 30 min, followed by incubation with 1% glutaraldehyde for 5 min. After washing with T-PBS several times, the EVs were observed by Transmission Electron Microscope at 80 kV. For the negative control, all the above procedures were followed except for primary antibody incubation. EVs were only incubated with 1% glutaraldehyde for 5 min. EVs size distribution or diameter was measured by ImageJ software (public domain free software version: java 1.8.0_172) after capture of EV images by TEM. Total Area(A) of EVs was measured upon nanometer (nm) scale. Later, the following equation was used for EVs diameter (D = nm) analysis.

$$A(nm) = \pi r^2 \ , \quad r = \sqrt{\frac{A}{\pi}} \ , \ \mathrm{D} = 2\mathrm{r}\ (\mathrm{nm})$$

### 3.2.3. Cell Culture

#### 3.2.3.1. Culture Media

CAO1/2-FP was prepared as previously reported [**Kazi et al., 2019**]. Briefly, DMEM-FBS-based adipogenic and osteogenic media were mixed in a 1:1 ratio and addressed as a combination of adipogenic and osteogenic media (CAO). The final concentrations of adipogenic and osteogenic inducers in CAO were: 550 nM dexamethasone (MP Biomedicals, Santa Ana, CA, USA; 1000 nM for adipogenic and 100 nM for osteogenic media), 0.5 µM IBMX (Wako, Osaka, Japan; adipogenic media), 1 µg/mL insulin (Sigma-Aldrich, St. Louis, MO, USA; adipogenic media), 10 mM β-glycerol phosphate (TCI, Tokyo, Japan; osteogenic media), and ascorbic acid 50 µg/mL (Wako, Osaka, Japan; osteogenic media). When the CAO was diluted twice with the DMEM-FBS, it was named CAO1/2. Subsequently, CAO1/2 was supplemented with FGF2 and PDGF-AA growth factors (PeproTech, Rocky Hill, NJ, USA) at 100 ng/mL; this culture medium was named CAO1/2-FP. To evaluate the effect of DPC-EVs on ASCs, EV-depleted FBS was administrated in all experiments.

#### 3.2.3.2. Isolation of DPCs

DPs were isolated from the C57BL/6-mouse vibrissa follicles in the anagen phase and then cultured in papilla cell growth medium (PCGM; Toyobo, Japan) at 37 °C with 5% $CO_2$. Outgrowing cells and DPCs were collected using Accutase™ (Innovative Cell Technologies, San Diego, CA, USA) and sub-cultured to propagate up to passage 4 ($p = 4$), then aliquoted and preserved in liquid $N_2$.

#### 3.2.3.3. Isolation of ASCs

Mouse adipose tissue was harvested from subcutaneous fat and inguinal fat pads, extensively washed with PBS, and finally minced. To remove clotted blood, muscle, or skin debris from the minced tissue, the fragments were centrifuged for 10 min at 300× *g* in a 50 ml conical tube. Floating tissue fragments were digested for 60 min at 37 °C in collagenase (Worthington Chemicals, Lakewood, NJ, USA) at a final concentration of 0.1%, while gently shaken. The digestion was stopped with DMEM-FBS, and the remaining samples were gently collected and filtered through a 100 mm cell strainer (BD Biosciences, San Jose, CA, USA). The cell supernatant was washed twice for 10 min and centrifuged twice for 5 min at 300× *g*. The pellets were resuspended in DMEM-FBS containing 1%

penicillin/streptomycin (Merck, St. Louis, MO, USA), and cells were counted. The cells were plated at a density of $1 \times 10^6$ cells in 100 mm culture dishes at 37 °C with 5% $CO_2$. After 24 h, non-adherent cells were removed. The adherent cells and ASCs were cultured with up to 80–90% confluence and passaged once with trypsin/EDTA (Thermo Fisher Scientific, Amarillo, TX, USA). For ASCs, passage 2 cells were used in the experiment.

Thawed ASC aliquots were cultured in CAO1/2-FP medium in a 6-well culture plate at a density of $7 \times 10^4$ cells/well. DPC-EVs were added to the culture medium on day three. On day six, the cells were dissociated with 0.25% trypsin/EDTA and inoculated in a low-adhesive 96-well plate (Prime surface; Sumitomo Bakelite, Tokyo, Japan) at $7 \times 10^3$ cells/well to form a three-dimensional (3D) structure (spheroid) over 3 days.

Unless stated otherwise, the ASCs in this study were cultured as spheroids. Spheroid culture was used since it is deemed more similar to in vivo models and important for maintaining stemness properties [**Marx, 2013**]. ASCs in a spheroid culture system were inoculated with 5 µg/mL of DPC-EVs (Fig. 11). The EV uptake assay was performed to ensure that the EVs were biologically active. EV uptake by ASCs was evaluated by incubating the cells with DPC-EVs for 48 h and then staining them with anti-CD63 antibodies to detect the incorporated EVs.

### 3.2.4. Oil O red and Alkaline phosphatase (ALP) staining:

To understand the capability of inducing differentiation of the CAO1/2 medium, ASCs were co-stained with Oil O red and ALP. Briefly, cells were fixed with 4% paraformaldehyde (PFA) for 10 min, washed in PBS, and then incubated in the substrate solution NBT/BCIP and TN Buffer for 30 min, in accordance with the manufacturer's instructions (Roach, Basel, Switzerland). The cells were then washed in the culture plate with Milli-Q water, rinsed with 60% isopropanol for 1 min, and stained with 0.3% Oil O red (Merck, St. Louis, MO, USA) for 30 min, rinsed with 60% isopropanol, and finally washed with Milli-Q water three times. For nuclei staining, the stained cells were incubated with 0.1% methyl green for 30 s.

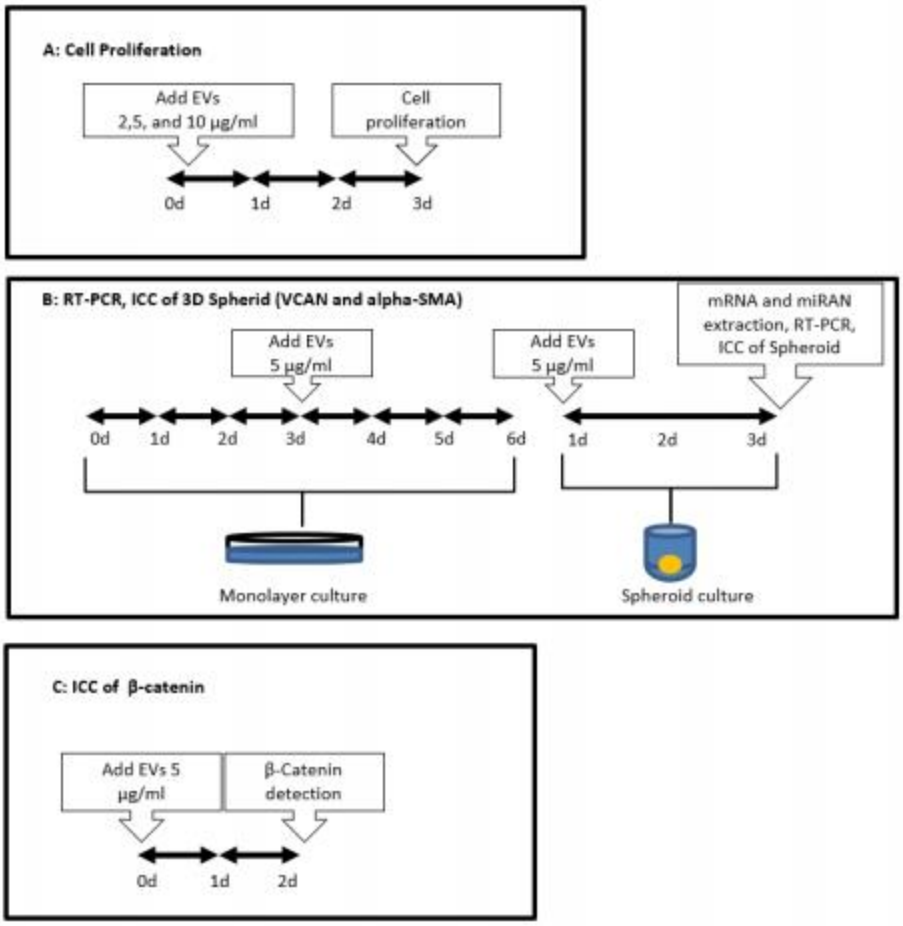


**Figure 11. The schematic figure represents experimental design**

### 3.2.5. Immunocytochemistry

The expression of VCN and ASMA was also confirmed by immunocytochemical analysis of spheroids (3D). DPC and ASCs with DPC-EVs spheroids were stained with anti-versican or α-SMA antibodies, followed by secondary antibodies conjugated with appropriate fluorescence labeling. To detect CTNB and PDGFa expression, ten thousand ASCs were inoculated in LAB-TEK II chamber slides (8 wells/slide; Thermo Fisher Scientific, Franklin Lakes, NJ, USA) for 2 and 7 days, respectively. The cells were then fixed with 4% PFA for 10 min and permeabilized with 0.1% Triton X-100 for 10 min at room temperature (25 °C). They were then blocked for 30 min with Block Ace (DS Pharma Biomedical, Osaka, Japan) in accordance with the manufacturer's instructions and treated with **a**nti-α-SMA antibody (MAB1420, R&D Systems, MN, USA), anti-PDGF-a polyclonal antibody (NBP2-99113

AF647, NOVUSBIO, Littleton, CO, USA), mouse anti-versican antibody (NBP2-22408 MAB, NOVUSBIO, Littleton, CO, USA), and anti-CD63 antibody (EPR21151, Abcam, Cambridge, UK) for the EV uptake assay. They were thoroughly washed with PBS containing 0.05% Tween-20 and reacted with secondary antibodies conjugated with Alexa Fluor 594 (ab150116), Alexa Fluor 647 (ab150115), and Alexa Fluor 488 (ab150113 and ab150077 for EVs), all conjugated with the secondary antibodies at a 1:600 dilution. DAPI Fluoromount-G (Southern Biotech, Birmingham, AL, USA) was used for nuclei staining. Fluorescent images were collected under a BZX-800 fluorescence microscope (Keyence, Osaka, Japan) and viewed with another fluorescence microscope (BX51N, Olympus, Shinjuku City, Tokyo, Japan), for Figures S1 and S2, with a digital monochrome camera DFC345FX (Leica Microsystems, Wetzlar, Germany, DE; all experiments related to Figures S1 and S2 were performed at Shimane University).

### 3.2.6. mRNA extraction and RT-PCR

Total RNA from the spheroids of each category was collected on day three using the RNeasy Mini Kit (Qiagen, Hilden, Germany). cDNA was prepared from the RNA using the QuantiTect reverse transcription kit (Qiagen, Venlo, The Netherlands). Real-time PCR analysis was performed to examine the gene expression levels (Table I) using the Thermal Cycler Dice® Real-Time System (TP 950; Takara Bio, Shiga, Japan) and cDNA template combined with the TB-Green Premix Ex Taq II kit (RR820A, Takara Bio, Shiga, Japan). β-actin was used as an internal control in all experiments.

### 3.2.7. miRNA extraction and RT-PCR

Total miRNA was collected from EVs and/or ASC EVs using the miRNeasy Mini Kit (Qiagen, Hilden, Germany). cDNA was prepared using the TaqMan™ MicroRNA Reverse Transcription Kit (Thermo Fisher Scientific, Waltham, MA, USA). The expression levels of hsa-mir-218-5p (assay ID: 000521), hsa-mir-214 (assay ID: 002293), hsa-miR-195 (assay ID: 000494), and internal control U6snRNA (assay ID: 001973) (Table-II) were analyzed using the Thermal Cycler Dice® Real-Time System (TP 800; Takara Bio, Shiga, Japan) and the TaqMan Fast Universal PCR Master Mix (2X) (4366072, Thermo Fisher Scientific, Waltham, MA, USA).

### 3.2.8. Protein concentration and Western blot

Dermal papilla cells and EVs were lysed in RIPA buffer (182-02451, Fujifilm, Japan). Protein concentrations were measured using a BCA protein assay kit (Thermo Fisher Scientific, Waltham, MA, USA). Extracted proteins from cells and EVs resolved in 10% SDS-PAGE were electrotransferred onto nitrocellulose membrane by semi-dry system. Then the blots were incubated in 0.3% BSA in TBST (Trish buffer saline with 0.1% Tween-20) for 1 h in room temperature. Specific primary antibodies **(**Rabbit mAb anti-CD63 #ab217345, rabbit mAb anti-TSG101#ab125011, rabbit mAb anti- beta Actin #ab115777, rabbit pAb anti-Hsp90#ab13495, and rabbit pAb anti-CYC1#ab137757**)** were added to the blots at 1:1000 dilution and incubated in 4 ℃ for overnight. The blots were washed in TBST and incubated in appropriate secondary antibody-conjugated horseradish peroxide (ab97051, Cambridge, UK). The blots were developed using chemiluminescence reagent (Luminata #WBLUR0500, Darmstadt, Germany).

### 3.2.9. Cell proliferation assay

MTT Cell Proliferation Assay Kit (Ab-211091, Cambridge, UK) was used for the cell proliferation assay. Manufacturer's instructions were followed. Briefly, the cell proliferation assay was performed at day three after EV inoculation in cell culture medium. The culture supernatant of adherent cells was carefully aspirated from the 12-well culture plate (TPP, Harlev, Denmark). A 1:1 ratio of serum-free media and MTT reagent mixture was added into each well. Subsequently, the culture plate was incubated at 37 °C for 3 h. After incubation, 1.5 volume of MTT solvent was added into the mixture in each well. After 15 min of orbital shaking, the culture plate was read with a plate reader (SH-9000lab, Corona Electrical, Hitachinaka-shi, Japan). Absorbance was measured at OD = 590 nm. The cell number of the sample plate was evaluated by comparison with the known cell number of the standard curve.

### 3.2.10. Statistical analysis

We performed a one-way analysis of variance (ANOVA) with post hoc Tukey HSD test (online web statistical calculator, https://astatsa.com/OneWay_Anova_with_TukeyHSD/)

for multiple groups, while Student's t-test was used for comparing two groups (Microsoft Excel).

### 3.3. Results

#### 3.3.1. Identification of DPC-EVs

To investigate the role of DPC-EVs, they were collected from DPCs, as described in the Materials and Methods section. Immuno-Electron Microscopy (IEM) analysis confirmed the presence of DPC-EVs in the conditioned medium, which was stained with an anti-CD63 surface marker conjugated with secondary antibodies and 10 nm gold particles (Fig 12A). No signal was detected in samples treated with 1% glutaraldehyde only (Fig 12B). Western blot analysis revealed the presence of ubiquitous EV markers, such as CD 63 and TSG101 (tumor susceptibility gene 101) protein, which are enriched in DPC-EVs compared with cell lysates (DPC). On the other hand, HSP90 (heat shock protein 90) and CYC-1 (cytochrome C), which belong to cell fractions, were depleted from EV (Fig 12C). The TEM images analysis indicates the average diameter of EVs was between 80 nm and 170 nm (Fig 12D). We performed an EV uptake assay to ensure that the EVs were biologically active. EV uptake by ASCs was evaluated by incubating the cells with DPC-EVs for 48 h and then staining them with anti-CD63 antibodies to detect the incorporated EVs (Fig 12E–G). CD63-positive signals were detected in the peri- and intra-nuclear areas of the incubated ASCs. We also examined the hair-related regulatory miRNAs—mir-214-5P, mir-218-5P, and mir-195-5P—in EVs derived from passage 4 (P4) or passage 5 (P5) DPCs. The keratinocyte proliferation inhibitor mir-214 was 5.3 times lower in P4 DPC-EVs than P5 DPC-EVs (Fig 12H), which was significant. The CTNB activator mir-218-5P was similarly detected in P4 and P5 DPC-EVs (Fig 12I). The CTNB regulatory mir-195-5P was 3.5 times higher in P4, suggesting significance (Fig 12J).

Taken together, isolated DPC-EVs were purified and biologically active, which was supported by Western blot, the sufficient uptake of ASCs, and the presence of miRNAs.

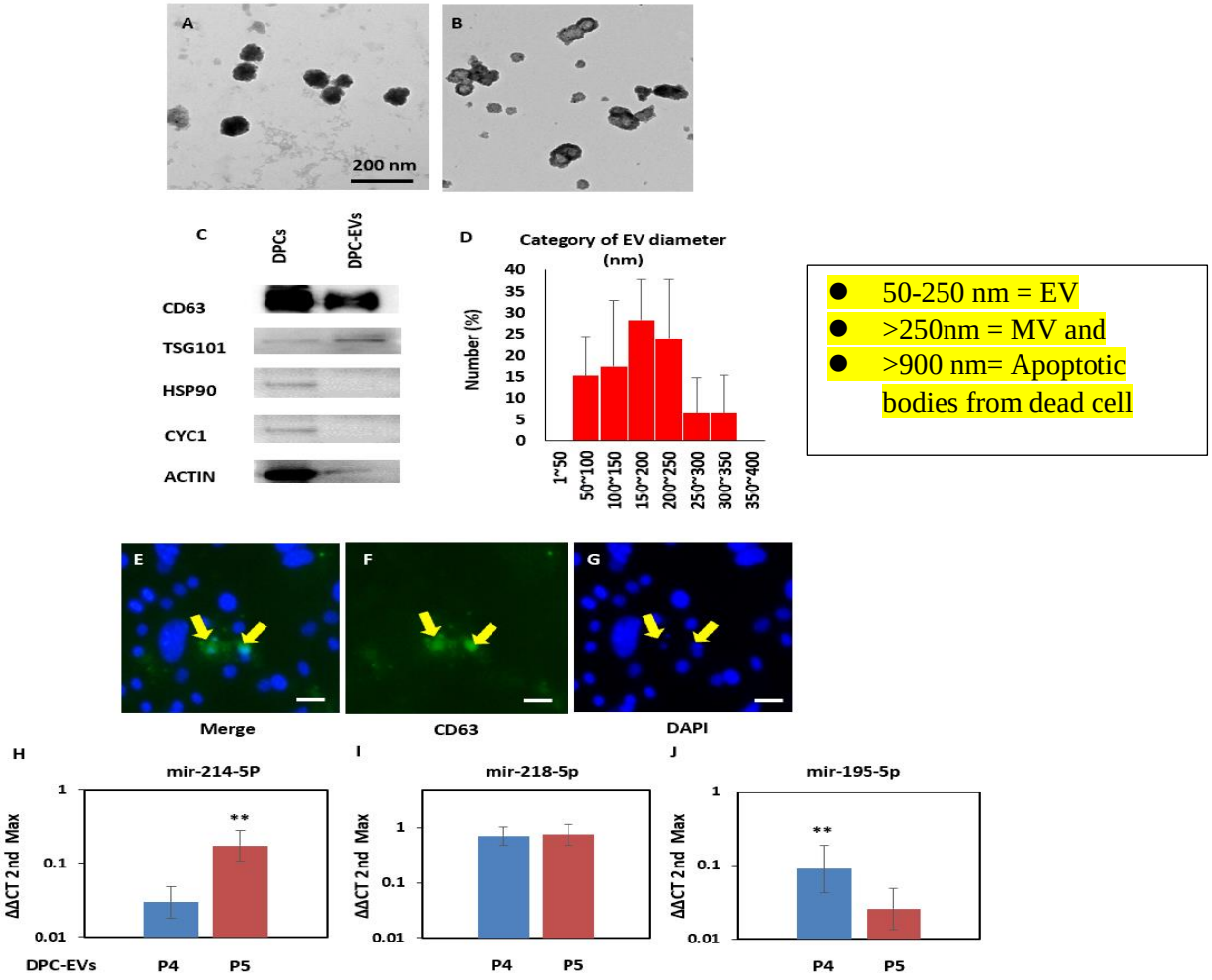


**Figure 12. Isolation and detection of dermal papilla cell-derived extracellular vesicles (DPC-EVs) by transmission electron microscopy (TEM) and quantitative PCR (qPCR) analysis of miRNA expression in DPC-EVs**

(**A**) DPC-EVs were detected by EV-specific anti-CD63 antibody followed by secondary antibodies conjugated with 10 nm gold beads (dense, black appearance). (**B**) As a negative control, DPC-EVs were stained with 1% glutaraldehyde, and no gold beads were attached. (**C**) DPCs and EVs were scrutinized by Western blot with specific antibodies. (**D**) The size distribution DPC-EVs were analyzed by ImageJ software 1.8.0_172. (**E**–**G**) Uptake of DPC-EVs by adipose-derived stem cells (ASCs). The yellow arrow indicates the EVs uptaken by ASCs; scale bar indicates 10 μm. (**H**–**J**) TaqMan-based real-time PCR analysis of exosomal mir-214-5P, mir-218-5p, and mir-195-5P in P4 and P5 DPC-EVs (n = 3). Data are presented as the mean value ± SD. ** $p < 0.01$.

### 3.3.2. Induction of Cell Proliferation and Inculcation of Hair Induction-Related Gene Expression in ASCs with DPC-EVs

It has been previously reported that mir-214 overexpression inhibited cell proliferation [**Ahmed et al.,2014**]. To circumvent the excessive influence of mir-214, P4 DPC-EVs, expressing lower mir-214-5P compared with P5 DPC-EVs, were selected for further experiments. First, we examined the effect of DPC-EVs on ASC proliferation. CAO1/2-FP increased ASC proliferation compared with DMEM-FBS. Surprisingly, 2 and 5 µg/mL and not 10 µg/mL DPC-EVs with CAO1/2-FP significantly enhanced cell proliferation compared with CAO1/2-FP only (Fig 13A). This suggests that 5 µg/mL of DPC-EVs with CAO1/2 is optimal for cell proliferation and hair inductive gene expression in ASCs. The DPC-EVs expressed mir-195 (Fig 12H). Hair induction-related genes in ASCs were significantly higher in CAO1/2-FP than in DMEM-FBS, even without DPC-EVs (Fig 13B–E). Real-time PCR analysis revealed that DPC-EVs significantly induced the expression of *vcan, ncam, α-sma,* and *opn* in ASCs of the spheroid culture system (Fig 13B–E). These data suggest that DPC-EVs with CAO1/2-FP (DPC-EVs/CAO1/2-FP) were biologically active and could transform ASCs into DPC-like cells with hair formation activity.

### 3.3.3. Transdifferentiation of ASCs into DPC-Like Cells through Incubation with DPC-EVs

DPCs can regenerate HFs in the mammalian hair cycle and express genes related to hair induction, such as *vcan*, *ctnb, α-sma*, *alp*, *opn*, *ncam,* and anagen inducer *leptin* (*lep*). We observed that the expression of vcan and ncam was, respectively, 1.3 and 3.6 times higher in ASCs with DPC-EVs compared with DPCs (Fig 14A, B). The genes ctnb and alp were expressed similarly in both cell types (Fig 14C, D). In contrast, expression of α-sma, opn, and leptin was significantly higher in DPCs than in ASCs with DPC-EVs (Fig 14E–G). The expression of VCAN (Fig 15A–F) and α-SMA (Fig 15G–L) was also confirmed by immunocytochemical analysis of spheroids (3D). DPCs and ASCs with DPC-EVs spheroids were stained with anti-VCN or α-SMA antibodies, followed by secondary antibodies conjugated with appropriate fluorescence labeling. As shown in Figure 15M and N, the expression of both proteins was almost consistent with the mRNA expression (Fig 14A, E).

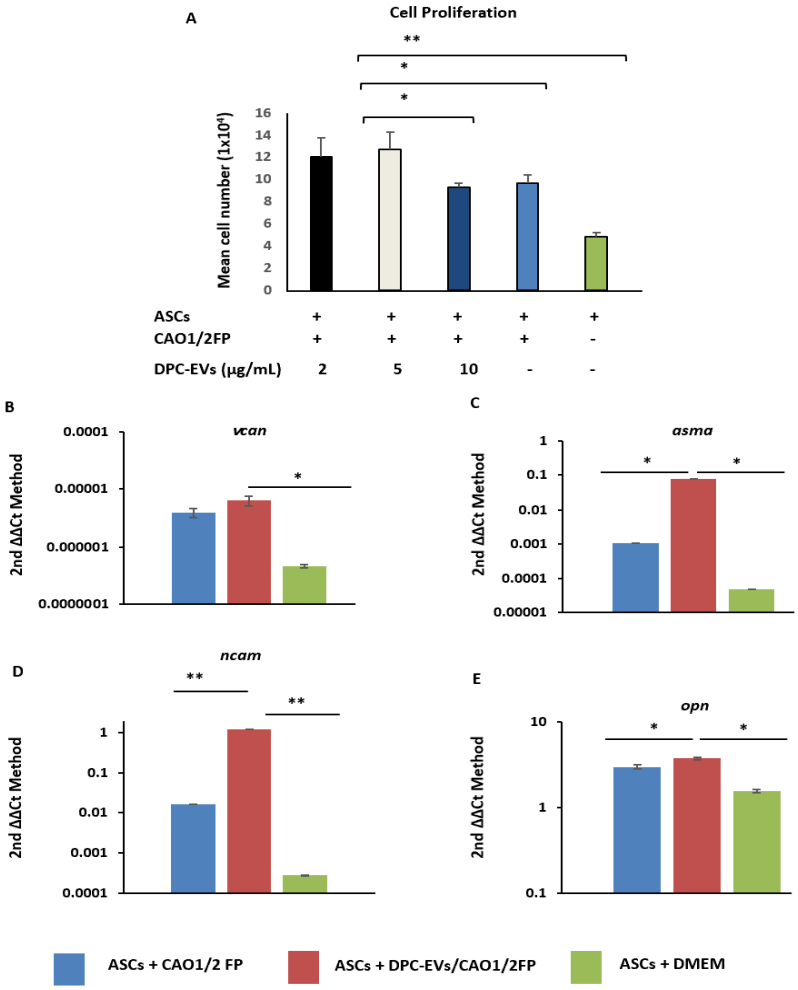


**Figure 13. Proliferation and hair-related gene expression of adipose-derived stem cells (ASCs) incubated with dermal papilla cell-derived extracellular vesicles (DPC-EVs) in combination with CAO1/2-FP.**

(**A**) Effect of DPC-EVs on ASC proliferation. (**B**–**E**) Expression of the DPC-related genes in the ASC spheroids. Spheroids were prepared in CAO1/2-FP medium ± DPC-EVs or DMEM-FBS. The DPC-related genes, *vcan* (***B***), *asma* (***C***), *ncam* (***D***), *and opn* (***E***), were analyzed with Taqman-based quantitative PCR. The average gene expression for each category was obtained from two independent experiments measured in triplicate, and data are presented as the mean value ± SD. * $p < 0.05$, and ** $p < 0.01$.

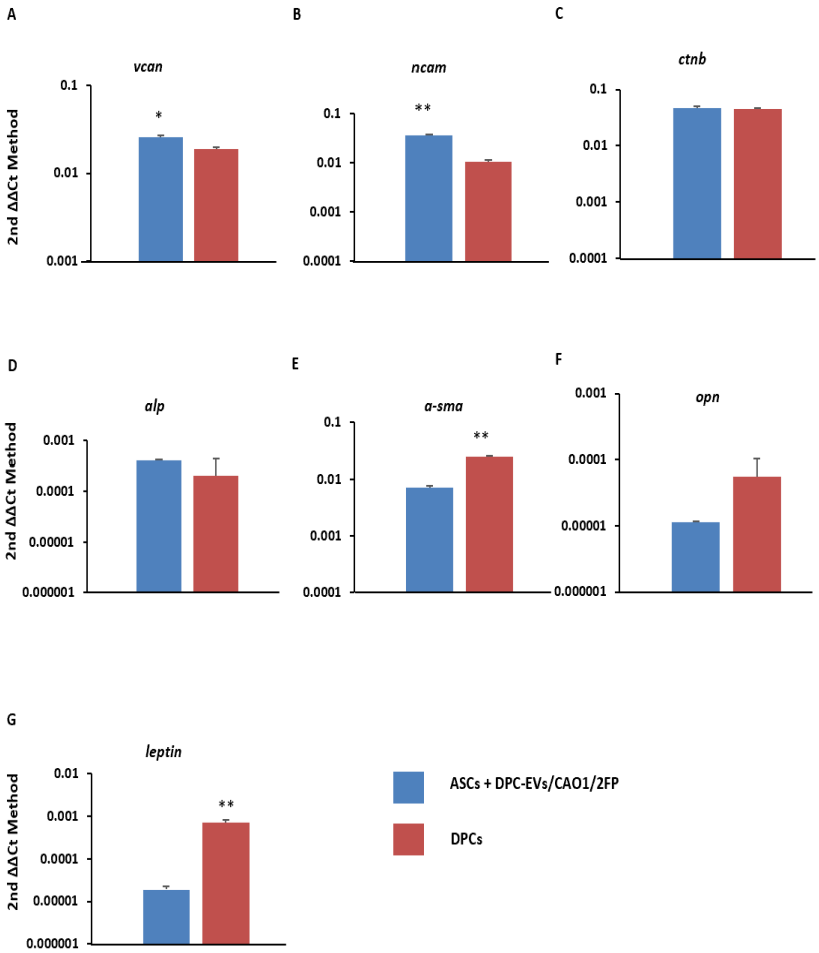


**Figure 14. Comparison of hair induction related genes**

**(A-G)** comparisons are illustrated between adipose-derived stem cells (ASCs) with DPC-EVs and dermal papilla cells (DPCs). Total RNA was isolated from each spheroid. The gene expression was analyzed with real-time PCR. The average gene expression for each category was obtained from three independent experiments measured in triplicate, and data are presented as the mean value ± SD (Error bars). * $p < 0.05$ and ** $p < 0.01$.

These data further support the ability of DPC-EVs to transdifferentiate ASCs into DPC-like cells.

### 3.3.4. Induction of CTNB pathway in ASCs through incubation with DPC-EVs and miRNAs

CTNB has been implicated as playing a pivotal role in HF development [**Han et al., 2018**]. If DPC-EVs can transdifferentiate ASCs into DPC-like cells, then CTNB will be induced in ASCs via incubation with DPC-EVs/CAO1/2-FP. To examine this possibility, we analyzed the expression of CNTB in ASCs and ASCs with DPC-EVs. CNTB was expressed in DPCs, as expected (Fig 16D–F). Monolayer ASCs, not spheroidal, under various conditions were utilized for staining. CTNB-positive cells were observed in ASCs cultured in CAP1/2FP and were also increased by the addition of DPC-EVs (Fig 16A–I, M). No signal was observed in the negative control (Fig 16J–L), and mean fluorescence intensities were consistent among the three groups (Fig 16N). It has been reported that mir-214 and mir-195-5P overexpression inhibits the canonical CTNB signaling pathway [**Ahmed et al., 2014, Zhu et al., 2018**]. To gain further insight into the DPC-EVs/CAO1/2-FP-induced transformation of ASCs, we compared the expression of these miRNAs between DPCs and ASCs with DPC-EVs/CAO1/2-FP. MicroRNAs were collected as described in Materials and Methods. Mir-214-5P and mir-195-5P were similarly expressed in both cell lines (Fig 16O, P). Notably, mir-218-5p, which has been reported to promote hair growth via upregulation of CTNB signaling [**Hu et al., 2020**], was significantly higher in ASCs with DPC-EVs than in DPCs alone (Fig 16Q). These results further suggest that DPC-EVs, in cooperation with CAP1/2FP, can transdifferentiate ASCs via the induction of the CTNB signaling pathway and a certain set of miRNAs—namely, mir-195.

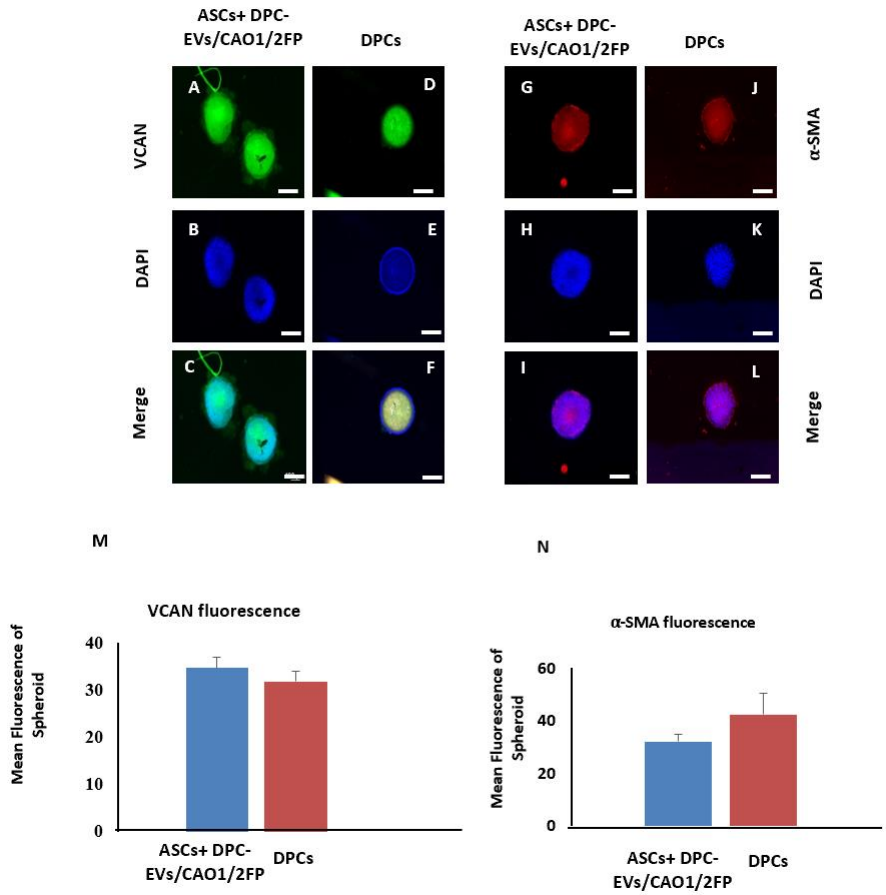


**Figure 15. Immunofluorescence microscopic analysis of VCAN and α-SMA in dermal papilla cells (DPCs) and adipose-derived stem cells (ASCs) with dermal papilla cell-derived extracellular vesicles (DPC-EVs) spheroids**

(**A**–**L**) Representative photograph of cells in each category, stained with anti- VCAN and α-SMA antibodies. (**M**, **N**) Quantitative histograms of VCAN and α-SMA fluorescence intensity in spheroids were made using the Image J software 1.8.0_172. The white scale bar represents 200 µm. Data are presented as the mean value ± SD and showed no significant difference between the two groups.

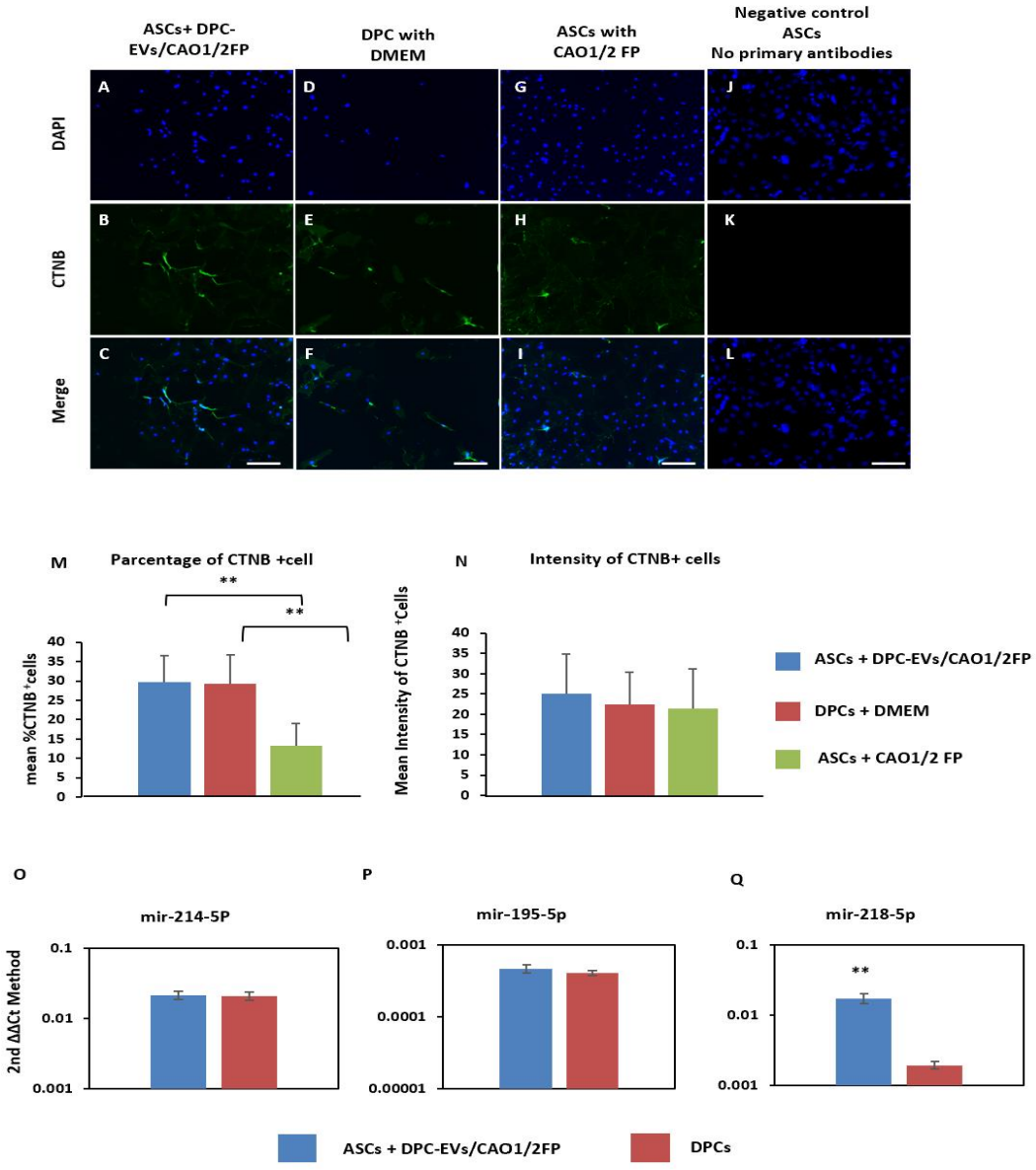


**Figure 16. Immunofluorescence microscopic analysis of CTNB in adipose-derived stem cells (ASCs) under various conditions**

(**A**–**C**) Immunofluorescence image of CTNB-positive cells in ASCs treated with DPC-EVs/CAO1/2-FP, (**D**–**F**) dermal papilla cells (DPCs) with DMEM-FBS, and (**G**–**I**) ASCs with CAO1/2-FP. (**J**–**L**) Negative control with no primary antibodies. (**M**) Percentage of CTNB-positive cells of total nuclei from randomly selected images. (**N**) Fluorescence intensity of CTNB-positive cells was quantified with Image J software 1.8.0_172. (**O**–**Q**) CTNB regulatory miRNA expression between DPCs and DPC-derived extracellular vesicles (DPC-EVs) treated ASCs with CAO1/2-FP, white scale bar represents 100 µm. Vertical bars represent the mean value ± SD, ** $p < 0.01$.

### 3.4. Discussion

In this study, the properties of DPC-EVs were characterized, and the potential of DPC-EVs and/or DPC-EVs/CAO1/2-FP to transfer the properties of DPCs into ASCs was also explored. Our study was composed of three sections: (1) identification and characterization of DPC-EVs, (2) comparison of hair-related/inductive gene expression between DPCs and ASCs with DPC-EVs, and (3) further characterization of ASCs with DPC-EVs by examining the CTNB signaling pathway.

First, we identified DPC-EVs and the hair-related miRNAs, mir-195-5p, mir-214-5p, and mir-218-5p in the DPC-EVs. The miRNA expression in P4 and P5 DPC-EVs was quantified by reverse transcription real-time PCR. As DPC-EVs contained mir-195, we hypothesized that it may enhance the expression of hair-inductive genes in ASCs, as well as increasing cell proliferation. However, it has been reported that miRNA expression changes in in vitro-cultured DPCs in a passage-dependent manner, and a high expression of one such miRNA, mir-195-5p, inhibited DPC proliferation when it was transfected [**Ahmed et al., 2014**]. Consistent with this, we revealed that exosomal miRNA expression varied between cell passage P4 and P5 (Fig 12H–J). In particular, mir-214 was significantly higher in P4 DPC-EVs than in P5 DPC-EVs. As mir-214 overexpression has been reported to be responsible for the reduction in HFs in developing skin, and for a delay in hair cycle progression during postnatal development [**Zhu et al., 2018**], DPC-EVs derived from the lower passage cells might have increased hair growth activities. Thus, we hypothesized that the lower expression of mir-214 in P4 DPS-EVs implies its potential role in providing DP-like properties to ASCs. In contrast, P4 and P5 DPC-EVs displayed similar mir-218-5p expression (Fig 12I). Hu et al. reported that mir-218-5p in EVs upregulates Ctnb and contributes to HF neogenesis [**Hu et al., 2020**]. However, P5 and P4 DPC-EVs might affect CTNB signaling and HF neogenesis differently. We have revealed that DPC-EVs, at concentrations as low as 2 μg/mL in combination with CAO1/2-FP, enhanced the proliferation of ASCs (Fig 13A). This strongly suggests that DPC-EVs are biologically active and affect the transformation of ASC properties into DP-like properties. Although DPC-EVs at the highest concentration (10 μg/mL) inhibited cell proliferation, high amounts of miRNAs such as mir-214, a known cell

inhibitory miRNA, might affect ASC proliferation. We are currently working on the influence of mir-214 on ASC proliferation and differentiation into DPC-like cells.

We previously reported that CAO1/2-FP medium (a combination of adipogenic and osteogenic inducers at low concentrations, with FGF-2 and PDGF-AA) was adequate for DPC in vitro culture and prevented DPC shrinkage by maintaining extracellular matrix components, versican, and other hair induction-related gene expression [**Kazi et al., 2019**]. We used CAO1/2-FP in the current study as a differentiation medium for ASCs. The key features of CAO1/2 medium were to prevent ASCs from differentiating into mature adipocytes or osteocytes (Fig 11Q–S) and enable ASCs to express hair-inductive genes such as vcan, α-sma, and ctnb (Fig 11K–P). EVs were endocytosed by recipient cells, and the RNA cargo in the EVs was transferred, which in turn altered the recipient cell gene expression profile and function [**Valadi et al.,2007; O'Brein et al., 2020**]. We analyzed the expression of hair induction-related genes expressed by DPCs in ASCs treated with CAO1/2-FP, DPC-EVs/CAP1/2FP, and DMEM-FBS. CAO1/2-FP seemed to be appropriate for ASCs and DPCs to transform ASCs into DPC-like cells. DPCs express characteristic genes, such as *vcan, sma, sox2, ctnb, alpl*, and so on, for HF morphogenesis into the postnatal hair cycle in mammals [**Kazi et al., 2019; Jahoda et al., 1991; Drislel et al., 2009**]. These genes are also expressed in non-DPCs, such as dermal sheath cells and dermal fibroblasts; however, combinations of these molecules are cell-type specific. For instance, DPCs are α-SMA-positive but DESMIN-negative, whereas dermal sheath cells are DESMIN-positive [**O'Brein et al., 2020**] and MSCs are SOX2-positive [**Marx 2013; Feng et al., 2015**], indicating that DPCs form heterologous populations. Nonetheless, we found that DPC-EVs enhanced vcan, ncam, and α-sma gene expression in ASCs, which are highly specific in the DPCs of anagen stage HFs (Fig 13B–E). When profiles of hair induction-related genes were compared between ASCs with DPC-EVs and DPCs, these were similar (Fig 14A–G). This indicates that DPC-EVs in combination with CAO1/2-FP can transform ASCs into DPC-like cells, which is also supported by immunocytochemical analyses of VCAN and ASMA (Fig 15A–N). CAO1/2-FP contains FGF-2 and PDGF-AA. FGF upregulates the expression of CTNB via Erk1/2 activation upon receptor binding [**Makiko et al., 2001**]. In contrast, PDGF-AA is a key molecule secreted as a paracrine factor from DPCs in the dermis, which promotes HF development and hair growth [**Festa et al., 2011**]. In this study, we found that

DPC-EVs in CAP1/2FP stimulated CTNB expression in ASCs (Fig 16M, N). DPC-EVs might work, but cooperatively with the growth factors in CAP1/2FP. CTNB plays an important role in cell cycle progression, cell proliferation, and gene regulation of Cyclind1 and c-Myc, as well as ctnb. Upon CTNB activation, it accumulates cytoplasm and translocate into the nucleus [**Lin et al., 2015**], and then transcriptionally regulates various events, such as the maintenance of the HF anagen phase [**Cao et al., 2021**].

Collectively, we demonstrated that DPC-EVs, especially prepared from P4 DPCs, could transdifferentiate ASCs into DPC-like cells in combination with CAP1/2FP, which was evidenced by the induction of hair growth-related genes via the CTNB pathway. Adipose tissue is rich in ASCs that can be easily collected from excess body fat in a relatively safer manner, compared with the collection of DPCs.

ASC-derived DPC-like cells might be useful in the treatment of hair-related diseases, such as alopecia, either independently or in combination with other available therapies. The limitations of our study, however, are a limited knowledge of miRNA expression, other than the miRNAs under examination, and an insufficient characterization of DPC-EVs in a passage-dependent manner. Further studies will be required to understand the therapeutic potential of DPC-EVs and ASC-derived DPC-like cells.

## Table II. Primer of RT PCR

| Primer Name | Forward Primer (5′-3′) | Reverse Primer (5′-3′) |
|---|---|---|
| versican | ACTAACCCATGCACTACATCAAG | ACTTTTCCAGACAGAGAGCCTT |
| α-smooth muscle actin | GGCACCACTGAACCCTAAGG | ACAATACCAGTTGTACGTCCAGA |
| alpl | GTGACTACCACTCGGGTGAAC | CTCTGGTGGCATCTCGTTATC |
| Osteopontine | TGCAAGCCCTTTGGCAATG | GCCGTCCATATAGCAGCCC |
| leptin | CCAGTTGGTAACAATGCCATGT | TTCAAAGCCGAGGCATTGTTT |
| beta-catenin (ctnb) | ATGGAGCCGGACAGAAAAGC | CTTGCCACTCAGGGAAGGA |
| ncam | AGAAATCAGCGTTGGAGAGTCC- | TCGTCATCATTCCACACCACT |
| CD44 | CACCATTGCCTCAACTGTGC | TTGTGGGCTCCTGAGTCTGA |
| CD45 | ACCACCAGGTGAATGTCAATTT | CTTGCTTTCCCTCGGTTCTTT |
| CD90 | TGCTCTCAGTCTTGCAGGTG | TGGATGGAGTTATCCTTGGTGTT |
| Pdgf-a | ACATGAGGGGACTCTGGGAA | ACAGTGAAGCCCAACAGCTT |
| Pdgf-b | ATTGTGCGAAAGAAGCCCATC | GGGTCACTACTGTCTCACACTT |
| beta-Actin | GGCTGTATTCCCCTCCATCG | CCAGTTGGTAACAATGCCATGT |

## Table III. Taqman microRNA sequences

| miRNA Name | Mature miRNA Sequence |
|---|---|
| mir-218-5p | UUGUGCUUGAUCUAACCAUGU |
| mir-214-5p | UGCCUGUCUACACUUGCUGUGC |
| mir-195-5p | UAGCAGCACAGAAAUAUUGGC |
| Internal control U6sn | GTGCTCGCTTCGGCAGCACATATACTAAAATTGGAACGATACAGA-GAAATTACATGGCCCCTGCGCAAGGATGACACGCAAATTCGTGAAGCGTTCCATATTTT |

# Chapter IV

# General Discussion

## 4.1. Signaling pathway of Osteogenic and Adipogenic Inducers

Dermal Papilla cells (DPC) easily lose their intrinsic properties especially hair inductive property while they are cultured in -vitro environment. Several methods have taken to subjugate the loss issue through propagation and maintenance of DPC in-vitro both monolayer and spheroid or 3D culture. It has been stated in previous researches that DPCs partially regain the hair inductive property if culturing under 3D condition. In this thesis, we showed a solution of one of drawbacks of 3D culture method, that is shrinkage of aggregated DPC. To get rid from this issue, we stimulated DPCs with factors known to induce adipogenic and/or osteogenic differentiation, because DPCs share unique gene expression profiles with adipocytes and osteocytes. Each individual inducer has significant roles to modulate signaling pathways specific for distinct cell lineage differentiation. Adipogenic inducers like dexamethasone, insulin and IBMX (3-isobutyle-1-methylxenthan) induce adipogenic differentiation of mesenchymal stem cell by activating PPAR-gamma and SCARA5 genes [**Lee et al., 2017; Takenaka et al., 2013**]. Besides, overexpression of SCARA5 downregulate FAK/ERK signaling pathway to inhibit phosphorylation for osteogenic differentiation [**Lee et al, 2017**]. Moreover, insulin and IBMX markedly enhance leptin production by PI3Kinase independent mechanism [**Zeigere et al, 2008**]. On the other hand, ascorbic acid is one of the osteogenic inducers and essential for production of type I collagen and consequently activating osteoblast specific gene via expression of osterix [**Xing et al, 2011**]. However, phosphate activation requires for osteoblast differentiation, in this regard β-glycerol phosphate with ascorbic acid facilitate free phosphate activation resulting osteopontin expression during osteogenic differentiation [**Beck et al, 2000**]. In addition, dexamethasone treatment with ascorbic acid and β-glycerophosphate can stimulate osteogenic differentiation of stem cells in vitro [**Langenbach et al, 2013**]. Thus, optimal combination of Adipogenic and Osteogenic Inducers may induce and balance the signaling pathways to enhance the DPC properties.

### 4.2. Interaction of FGF2 and PDGF AA with CAO1/2 medium

In this study, we showed that addition of FGF-2 and PDGF-AA augmented versican promoter-driven GFP fluorescence of the spheroids made from DPCs cultured in CAO1/2 and also prevented spheroid shrinkage. The shrinkage of the spheroids causes cell-death of the spheroids inside and results in fading of DPC function. FGF-2 and PDGF-AA would maintain the spheroid size by supporting cell-survival and stimulating the production of Runx2, a transcription factor important for osteoblast differentiation [**Komori, 2019**]. Runx2 modulates proteoglycan expression such as vcan via FGF/MAPK/Runx2 signaling pathway [**Teplyuk et al, 2009**], which would contribute to prevent shrinkage of the spheroids working by filling the space among DPCs. Runx2 is activated through extracellular signal-regulated kinase (ERK) which can be stimulated via a signaling pathway mediated by integrins associated with collagen type I. Ascorbic acid accelerates collagen synthesis, and FGF and dexamethasone induce Runx2 expression. Moreover, addition of PDGF-AA augmented Runx2 protein expression in a BMP-Smad1/5/8-dependent manner [**Li et al, 2014**]. Therefore, most of ingredients of CAO1/2-FP would function to activate Runx2-mediated pathway, which would stimulate DPCs produce the hair induction related genes and protein to the levels similar to those of the intact dermal papillae.

### 4.3. miRNA play pivotal role to translocate β-catenin

Recently, extracellular vesicle (EV)-mediated cell differentiation has gained attention in developmental biology due to genetic exchange between donor cells and recipient cells via transfer of mRNA and miRNA. Which altered the recipient cell gene expression profile and function [**Valadi et al, 2007**]. EVs, also known as exosomes, play a role in maintaining paracrine cell communication and can induce cell proliferation and differentiation. Real-time PCR analysis and immunostaining revealed that DPC-EVs administered with the CAO1/2-FP promoted to induce DPC-like properties in ASCs. In-vivo mir-214 overexpression has been reported to be responsible for the reduction in HFs in developing skin, and for a delay in hair cycle progression during postnatal development [**Ahmed et al, 2014**], on the other hand, mir-218-5P overexpress attuned anagen hair follicle and upregulate β-Catenin expression [**Hu et al, 2020**]. Wnt/β-catenin signaling pathway is indispensable for activate vcan and to form dermal condensation which is the initial morphological change of hair

follicle neogenesis [**Yang et al, 2012; Tsai et al, 2014**]. Here, we found that miRNA expression patterns varied in DPC-EVs around passage 4 (P4) of DPC culture, which is known to be a critical time point to lose hair inductivity of the cells [**Jahoda et al., 1984**]. We hypothesized that miRNA may enhance the expression of hair-inductive genes in ASCs, as well as increasing cell proliferation. However, it has been reported that miRNA expression changes in-cultured DPCs in a passage-dependent manner, and a high expression of one such miRNA, mir-195-5p, inhibited DPC proliferation and inactivate β-catenin [**Zhu et al,2018**]. Briefly, DPC-EVs at early passage activating β-catenin whose activity may enhance through CAO1/2-FP medium.

Wnt signaling stabilizes β-catenin, which is of prime importance for activation and maintenance of DPC-specific properties including hair inductive ability in cultured DPCs. To find out the ideal culture condition, CAOP1/2-FP should be supplemented with Wnt and BMP proteins at optimal concentration in fine controlling with miRNA like mir-218-5P. These findings would provide us the better method to obtain a large amount of functional DPCs in vitro, which helps understanding hair disorders and being used for cell-based therapy.

## References


Ahmed, M. I., Alam, M., Emelianov, V. U., Poterlowicz, K., Patel, A., Sharov, A. A., Mardaryev, A. N., & Botchkareva, N. V. (2014). MicroRNA-214 controls skin and hair follicle development by modulating the activity of the Wnt pathway. *The journal of cell biology*, *207*(4), 549–567. https://doi.org/10.1083/jcb.201404001

Banka, N., Bunagan, M. J., & Shapiro, J. (2013). Pattern hair loss in men: diagnosis and medical treatment. *Dermatologic clinics*, *31*(1), 129–140. https://doi.org/10.1016/j.det.2012.08.003

Beck, G. R., Jr, Zerler, B., & Moran, E. (2000). Phosphate is a specific signal for induction of osteopontin gene expression. *Proceedings of the national academy of sciences of the United States of America*, *97*(15), 8352–8357. https://doi.org/10.1073/pnas.140021997

Botchkarev, V. A., & Kishimoto, J. (2003). Molecular control of epithelial-mesenchymal interactions during hair follicle cycling. *The journal of investigative dermatology. Symposium proceedings*, *8*(1), 46–55. https://doi.org/10.1046/j.1523-1747.2003.12171.x

Burgess, W. H., & Maciag, T. (1989). The heparin-binding (fibroblast) growth factor family of proteins. *Annual review of biochemistry*, *58*, 575–606. https://doi.org/10.1146/annurev.bi.58.070189.003043

Cao, L., Tian, T., Huang, Y., Tao, S., Zhu, X., Yang, M., Gu, J., Feng, G., Ma, Y., Xia, R., Xu, W., & Wang, L. (2021). Neural progenitor cell-derived nanovesicles promote hair follicle growth via miR-100. *Journal of nanobiotechnology*, *19*(1), 20. https://doi.org/10.1186/s12951-020-00757-5

Chueh, S. C., Lin, S. J., Chen, C. C., Lei, M., Wang, L. M., Widelitz, R., Hughes, M. W., Jiang, T. X., & Chuong, C. M. (2013). Therapeutic strategy for hair regeneration: hair cycle activation, niche environment modulation, wound-induced follicle neogenesis, and stem cell engineering. *Expert opinion on biological therapy*, *13*(3), 377–391. https://doi.org/10.1517/14712598.2013.739601

Couchman J. R. (1993). Hair follicle proteoglycans. *The journal of investigative dermatology*,*101*(1 Suppl), 60S–64S. https://doi.org/10.1111/1523-1747.ep12362642

Driskell, R. R., Giangreco, A., Jensen, K. B., Mulder, K. W., & Watt, F. M. (2009). Sox2 positive dermal papilla cells specify hair follicle type in mammalian epidermis. *Development*, *136*(16), 2815–2823. https://doi.org/10.1242/dev.038620

Eslaminejad, M. B., Fani, N., & Shahhoseini, M. (2013). Epigenetic regulation of osteogenic and chondrogenic differentiation of mesenchymal stem cells in culture. *Cell journal*, *15*(1), 1–10.

Feng, R., & Wen, J. (2015). Overview of the roles of Sox2 in stem cell and development. *Biological chemistry*, *396*(8), 883–891. https://doi.org/10.1515/hsz-2014-0317

Festa, E., Fretz, J., Berry, R., Schmidt, B., Rodeheffer, M., Horowitz, M., & Horsley, V. (2011). Adipocyte lineage cells contribute to the skin stem cell niche to drive hair cycling. *Cell*, *146*(5), 761–771. https://doi.org/10.1016/j.cell.2011.07.019

Han, L., Liu, B., Chen, X., Chen, H., Deng, W., Yang, C., Ji, B., & Wan, M. (2018). Activation of Wnt/β-catenin signaling is involved in hair growth-promoting effect of 655-nm red light and LED in in vitro culture model. *Lasers in medical science*, *33*(3), 637–645. https://doi.org/10.1007/s10103-018-2455-3

Hardy M. H. (1992). The secret life of the hair follicle. *Trends in genetics: TIG*, *8*(2), 55–61. https://doi.org/10.1016/0168-9525(92)90350-d

Higgins, C. A., Chen, J. C., Cerise, J. E., Jahoda, C. A., & Christiano, A. M. (2013). Microenvironmental reprogramming by three-dimensional culture enables dermal papilla cells to induce de novo human hair-follicle growth. *Proceedings of the national academy of science of the United States of America*, *110*(49), 19679–19688. https://doi.org/10.1073/pnas.1309970110

Hu, S., Li, Z., Lutz, H., Huang, K., Su, T., Cores, J., Dinh, P. C., & Cheng, K. (2020). Dermal exosomes containing miR-218-5p promote hair regeneration by regulating β-catenin signaling. *Science advances*, *6*(30), eaba1685. https://doi.org/10.1126/sciadv.aba1685

Iguchi, M., Aiba, S., Yoshino, Y., & Tagami, H. (2001). Human follicular papilla cells carry out nonadipose tissue production of leptin. *The journal of investigative dermatology*, *117*(6), 1349–1356. https://doi.org/10.1046/j.0022-202x.2001.01606.x

Iida, M., Ihara, S., & Matsuzaki, T. (2007). Hair cycle-dependent changes of alkaline phosphatase activity in the mesenchyme and epithelium in mouse vibrissal follicles. *Development, growth & differentiation*, *49*(3), 185–195. https://doi.org/10.1111/j.1440-169X.2007.00907.x

Inamatsu, M., Tochio, T., Makabe, A., Endo, T., Oomizu, S., Kobayashi, E., & Yoshizato, K. (2006). Embryonic dermal condensation and adult dermal papilla induce hair follicles in adult glabrous epidermis through different mechanisms. *Development, growth & differentiation*, *48*(2),

73–86. https://doi.org/10.1111/j.1440-169X.2006.00848.x

Jacobson C. M. (1966). A comparative study of the mechanisms by which X-irradiation and genetic mutation cause loss of vibrissae in embryo mice. *Journal of embryology and experimental morphology*, *16*(2), 369–379.

Jahoda C. A. (1998). Cellular and developmental aspects of androgenetic alopecia. *Experimental dermatology*, *7*(5), 235–248.

Jahoda, C. A., & Reynolds, A. J. (2001). Hair follicle dermal sheath cells: unsung participants in wound healing. *Lancet*, *358*(9291), 1445–1448. https://doi.org/10.1016/S0140-6736(01)06532-1

Jahoda, C. A., Horne, K. A., & Oliver, R. F. (1984). Induction of hair growth by implantation of cultured dermal papilla cells. *Nature*, *311*(5986), 560–562. https://doi.org/10.1038/311560a0

Jahoda, C. A., Reynolds, A. J., Chaponnier, C., Forester, J. C., & Gabbiani, G. (1991). Smooth muscle alpha-actin is a marker for hair follicle dermis in vivo and in vitro. *Journal of cell science*, *99*, 627–636. https://doi.org/10.1242/jcs.99.3.627

Jahoda, C. A., & Oliver, R. F. (1984). Vibrissa dermal papilla cell aggregative behaviour in vivo and in vitro. *Journal of embryology and experimental morphology*, *79*, 211–224.

Jung, Y. J., Kim, H. K., Cho, Y., Choi, J. S., Woo, C. H., Lee, K. S., Sul, J. H., Lee, C. M., Han, J., Park, J. H., Jo, D. G., & Cho, Y. W. (2020). Cell reprogramming using extracellular vesicles from differentiating stem cells into white/beige adipocytes. *Science advances*, *6*(13), eaay6721. https://doi.org/10.1126/sciadv.aay6721

Lee, H., Lee, Y. J., Choi, H., Seok, J. W., Yoon, B. K., Kim, D., Han, J. Y., Lee, Y., Kim, H. J., & Kim, J. W. (2017). SCARA5 plays a critical role in the commitment of mesenchymal stem cells to adipogenesis. *Scientific reports*, *7*(1), 14833. https://doi.org/10.1038/s41598-017-12512-2

Kazi, T., Niibe, I., Nishikawa, A., & Matsuzaki, T. (2020). Optimal stimulation toward the dermal papilla lineage can be promoted by combined use of osteogenic and adipogenic inducers. *FEBS open bio*, *10*(2), 197–210. https://doi.org/10.1002/2211-5463.12763

Kim, S. P., Ha, J. M., Yun, S. J., Kim, E. K., Chung, S. W., Hong, K. W., Kim, C. D., & Bae, S. S. (2010). Transcriptional activation of peroxisome proliferator-activated receptor-gamma requires activation of both protein kinase A and Akt during adipocyte differentiation. *Biochemical and biophysical research communications*, *399*(1), 55–59. https://doi.org/10.1016/j.bbrc.2010.07.038

Kim, W. K., Jung, H., Kim, D. H., Kim, E. Y., Chung, J. W., Cho, Y. S., Park, S. G., Park, B. C., Ko, Y., Bae, K. H., & Lee, S. C. (2009). Regulation of adipogenic differentiation by LAR tyrosine phosphatase in human mesenchymal stem cells and 3T3-L1 preadipocytes. *Journal of cell science*, *122*(Pt 22), 4160–4167. https://doi.org/10.1242/jcs.053009

Kishimoto, J., Ehama, R., Wu, L., Jiang, S., Jiang, N., & Burgeson, R. E. (1999). Selective activation of the versican promoter by epithelial- mesenchymal interactions during hair follicle development. *Proceedings of the national academy of science of the United States of America*, *96*(13), 7336–7341. https://doi.org/10.1073/pnas.96.13.7336

Langenbach, F., & Handschel, J. (2013). Effects of dexamethasone, ascorbic acid and β-glycerophosphate on the osteogenic differentiation of stem cells in vitro. *Stem cell research & therapy*, *4*(5), 117. https://doi.org/10.1186/scrt328.

Lee, H., Lee, Y. J., Choi, H., Seok, J. W., Yoon, B. K., Kim, D., Han, J. Y., Lee, Y., Kim, H. J., & Kim, J. W. (2017). SCARA5 plays a critical role in the commitment of mesenchymal stem cells to adipogenesis. *Scientific reports*, *7*(1), 14833. https://doi.org/10.1038/s41598-017-12512-2

Lenoir N. (2000). Europe confronts the embryonic stem cell research challenge. *Science*, *287*(5457), 1425–1427. https://doi.org/10.1126/science.287.5457.1425

Li, A., Xia, X., Yeh, J., Kua, H., Liu, H., Mishina, Y., Hao, A., & Li, B. (2014). PDGF-AA promotes osteogenic differentiation and migration of mesenchymal stem cell by down-regulating PDGFRα and derepressing BMP-Smad1/5/8 signaling. *PloS one*, *9*(12), e113785. https://doi.org/10.1371/journal.pone.0113785.

Lin, W. H., Xiang, L. J., Shi, H. X., Zhang, J., Jiang, L. P., Cai, P. T., Lin, Z. L., Lin, B. B., Huang, Y., Zhang, H. L., Fu, X. B., Guo, D. J., Li, X. K., Wang, X. J., & Xiao, J. (2015). Fibroblast growth factors stimulate hair growth through β-catenin and Shh expression in C57BL/6 mice. *BioMed research international*, *2015*, 730139. https://doi.org/10.1155/2015/730139

Lundgren, M., Burén, J., Ruge, T., Myrnäs, T., & Eriksson, J. W. (2004). Glucocorticoids down-regulate glucose uptake capacity and insulin-signaling proteins in omental but not subcutaneous human adipocytes. *The journal of clinical endocrinology and metabolism*, *89*(6), 2989–2997. https://doi.org/10.1210/jc.2003-031157

Iguchi, M., Aiba, S., Yoshino, Y., & Tagami, H. (2001). Human follicular papilla cells carry out nonadipose tissue production of leptin. *The journal of investigative dermatology*, *117*(6), 1349–

1356. https://doi.org/10.1046/j.0022-202x.2001.01606.x

Marx V. (2013). Cell culture: a better brew. *Nature*, *496*(7444), 253–258. https://doi.org/10.1038/496253a

Kiso, M., Hamazaki, T. S., Itoh, M., Kikuchi, S., Nakagawa, H., & Okochi, H. (2015). Synergistic effect of PDGF and FGF2 for cell proliferation and hair inductive activity in murine vibrissal dermal papilla in vitro. *Journal of dermatological science*, *79*(2), 110–118. https://doi.org/10.1016/j.jdermsci.2015.04.007

Messenger, A. G., Elliott, K., Temple, A., & Randall, V. A. (1991). Expression of basement membrane proteins and interstitial collagens in dermal papillae of human hair follicles. *The journal of investigative dermatology*, *96*(1), 93–97. https://doi.org/10.1111/1523-1747.ep12515907

Higgins, C. A., Chen, J. C., Cerise, J. E., Jahoda, C. A., & Christiano, A. M. (2013). Microenvironmental reprogramming by three-dimensional culture enables dermal papilla cells to induce de novo human hair-follicle growth. *Proceedings of the national academy of science of the United States of America*, *110*(49), 19679–19688. https://doi.org/10.1073/pnas.1309970110

Millar S. E. (2002). Molecular mechanisms regulating hair follicle development. *The Journal of investigative dermatology*, *118*(2), 216–225. https://doi.org/10.1046/j.0022-202x.2001.01670.x

Mizuno H. (2009). Adipose-derived stem cells for tissue repair and regeneration: ten years of research and a literature review. *Journal of nippon medical school (Nippon Ika Daigaku zasshi)*, *76*(2), 56–66. https://doi.org/10.1272/jnms.76.56

Narayanan, R., Huang, C. C., & Ravindran, S. (2016). Hijacking the Cellular Mail: Exosome Mediated Differentiation of Mesenchymal Stem Cells. *Stem cells international*, *2016*, 3808674. https://doi.org/10.1155/2016/3808674

Ohyama, M., Kobayashi, T., Sasaki, T., Shimizu, A., & Amagai, M. (2012). Restoration of the intrinsic properties of human dermal papilla in vitro. *Journal of cell science*, *125*(Pt 17), 4114–4125. https://doi.org/10.1242/jcs.105700

Oliver R. F. (1967). The experimental induction of whisker growth in the hooded rat by implantation of dermal papillae. *Journal of embryology and experimental morphology*, *18*(1), 43–51.

Ostman, J., Arner, P., Engfeldt, P., & Kager, L. (1979). Regional differences in the control of lipolysis in human adipose tissue. *Metabolism: clinical and experimental*, *28*(12), 1198–1205. https://doi.org/10.1016/0026-0495(79)90131-8

O'Brien, K., Breyne, K., Ughetto, S., Laurent, L. C., & Breakefield, X. O. (2020). RNA delivery by extracellular vesicles in mammalian cells and its applications. *Nature reviews. Molecular cell biology*, *21*(10), 585–606. https://doi.org/10.1038/s41580-020-0251-y

Pawitan J. A. (2014). Prospect of stem cell conditioned medium in regenerative medicine. *BioMed research international*, *2014*, 965849. https://doi.org/10.1155/2014/965849

Peerani, R., Rao, B. M., Bauwens, C., Yin, T., Wood, G. A., Nagy, A., Kumacheva, E., & Zandstra, P. W. (2007). Niche-mediated control of human embryonic stem cell self-renewal and differentiation. *The EMBO journal*, *26*(22), 4744–4755. https://doi.org/10.1038/sj.emboj.7601896

Pisansarakit, P., du Cros, D. L., & Moore, G. P. (1991). Cultivation of mesenchymal cells derived from the skin and hair follicles of the sheep: the involvement of peptide factors in growth regulation. *Archives of dermatological research*, *283*(5), 321–327. https://doi.org/10.1007/BF00376621

Rajendran, R. L., Gangadaran, P., Bak, S. S., Oh, J. M., Kalimuthu, S., Lee, H. W., Baek, S. H., Zhu, L., Sung, Y. K., Jeong, S. Y., Lee, S. W., Lee, J., & Ahn, B. C. (2017). Extracellular vesicles derived from MSCs activates dermal papilla cell in vitro and promotes hair follicle conversion from telogen to anagen in mice. *Scientific reports*, *7*(1), 15560. https://doi.org/10.1038/s41598-017-15505-3

Robinson, M., Reynolds, A. J., & Jahoda, C. A. (1997). Hair cycle stage of the mouse vibrissa follicle determines subsequent fiber growth and follicle behavior in vitro. *The journal of investigative dermatology*, *108*(4), 495–500. https://doi.org/10.1111/1523-1747.ep12289730

Schmidt, B., & Horsley, V. (2012). Unravelling hair follicle-adipocyte communication. *Experimental dermatology*, *21*(11), 827–830. https://doi.org/10.1111/exd.12001

Shinomura, T., Nishida, Y., Ito, K., & Kimata, K. (1993). cDNA cloning of PG-M, a large chondroitin sulfate proteoglycan expressed during chondrogenesis in chick limb buds. Alternative spliced multi forms of PG-M and their relationships to versican. *The journal of biological chemistry*, *268*(19), 14461–14469.

Soma, T., Tajima, M., & Kishimoto, J. (2005). Hair cycle-specific expression of versican in human hair follicles. *Journal of dermatological science*, *39*(3), 147–154. https://doi.org/10.1016/j.jdermsci.2005.03.010

Stenderup, K., Justesen, J., Clausen, C., & Kassem, M. (2003). Aging is associated with decreased maximal life span and accelerated senescence of bone marrow stromal cells. *Bone*, *33*(6), 919–926. https://doi.org/10.1016/j.bone.2003.07.005

Takahashi, K., & Yamanaka, S. (2006). Induction of pluripotent stem cells from mouse embryonic and adult fibroblast cultures by defined factors. *Cell*, *126*(4), 663–676. https://doi.org/10.1016/j.cell.2006.07.024

Takenaka, Y., Inoue, I., Nakano, T., Shinoda, Y., Ikeda, M., Awata, T., & Katayama, S. A. (2013). Novel Splicing Variant of Peroxisome Proliferator-Activated Receptor-γ (Pparγ1sv) Cooperatively Regulates Adipocyte Differentiation with Pparγ2. *PLoS One*, 8(6), e65583. https://doi.org/10.1371/journal.pone.0065583

Teplyuk, N. M., Haupt, L. M., Ling, L., Dombrowski, C., Mun, F. K., Nathan, S. S., Lian, J. B., Stein, J. L., Stein, G. S., Cool, S. M., & van Wijnen, A. J. (2009). The osteogenic transcription factor Runx2 regulates components of the fibroblast growth factor/proteoglycan signaling axis in osteoblasts. *Journal of cellular biochemistry*, *107*(1), 144–154. https://doi.org/10.1002/jcb.22108

Tsai, S. Y., Sennett, R., Rezza, A., Clavel, C., Grisanti, L., Zemla, R., Najam, S., & Rendl, M. (2014). Wnt/β-catenin signaling in dermal condensates is required for hair follicle formation. *Developmental biology*, *385*(2), 179–188. https://doi.org/10.1016/j.ydbio.2013.11.023

Yu, D. W., Yang, T., Sonoda, T., Gong, Y., Cao, Q., Gaffney, K., Jensen, P. J., Freedberg, I. M., Lavker, R. M., & Sun, T. T. (2001). Osteopontin gene is expressed in the dermal papilla of pelage follicles in a hair-cycle-dependent manner. *The journal of investigative dermatology*, *117*(6), 1554–1558. https://doi.org/10.1046/j.0022-202x.2001.01568.x

Valadi, H., Ekström, K., Bossios, A., Sjöstrand, M., Lee, J. J., & Lötvall, J. O. (2007). Exosome-mediated transfer of mRNAs and microRNAs is a novel mechanism of genetic exchange between cells. *Nature cell biology*, *9*(6), 654–659. https://doi.org/10.1038/ncb1596

Westgate, G. E., Messenger, A. G., Watson, L. P., & Gibson, W. T. (1991). Distribution of proteoglycans during the hair growth cycle in human skin. *The journal of investigative dermatology*, *96*(2), 191–195. https://doi.org/10.1111/1523-1747.ep12461019

Wollin, L., Wex, E., Pautsch, A., Schnapp, G., Hostettler, K. E., Stowasser, S., & Kolb, M. (2015). Mode of action of nintedanib in the treatment of idiopathic pulmonary fibrosis. *The european respiratory journal*, *45*(5), 1434–1445. https://doi.org/10.1183/09031936.00174914

Xing, W., Pourteymoor, S., & Mohan, S. (2011). Ascorbic acid regulates osterix expression in osteoblasts by activation of prolyl hydroxylase and ubiquitination-mediated proteosomal degradation pathway. *Physiological genomics*, *43*(12), 749–757. https://doi.org/10.1152/physiolgenomics.00229.2010

Yamagata, M., & Kimata, K. (1994). Repression of a malignant cell-substratum adhesion phenotype by inhibiting the production of the anti-adhesive proteoglycan, PG-M/versican. *Journal of cell science*, *107*, 2581–2590. https://doi.org/10.1242/jcs.107.9.2581

Yang, Y., Li, Y., Wang, Y., Wu, J., Yang, G., Yang, T., Gao, Y., & Lu, Y. (2012). Versican gene: regulation by the β-catenin signaling pathway plays a significant role in dermal papilla cell aggregative growth. *Journal of dermatological science, 68*(3), 157–163. https://doi.org/10.1016/j.jdermsci.2012.09.011

Young F. E. (2000). A time for restraint. *Science*, *87*(5457), 1424. https://doi.org/10.1126/science.287.5457.1424

Yu, D. W., Yang, T., Sonoda, T., Gong, Y., Cao, Q., Gaffney, K., Jensen, P. J., Freedberg, I. M., Lavker, R. M., & Sun, T. T. (2001). Osteopontin gene is expressed in the dermal papilla of pelage follicles in a hair-cycle-dependent manner. *The journal of investigative dermatology*, *117*(6), 1554–1558. https://doi.org/10.1046/j.0022-202x.2001.01568.x

Yu, J., Tu, Y. K., Tang, Y. B., & Cheng, N. C. (2014). Stemness and transdifferentiation of adipose-derived stem cells using L-ascorbic acid 2-phosphate-induced cell sheet formation. *Biomaterials*, *35*(11), 3516–3526. https://doi.org/10.1016/j.biomaterials.2014.01.015

Zeigerer, A., Rodeheffer, M. S., McGraw, T. E., & Friedman, J. M. (2008). Insulin regulates leptin secretion from 3T3-L1 adipocytes by a PI 3 kinase independent mechanism. *Experimental cell research*, *314*(11-12), 2249–2256. https://doi.org/10.1016/j.yexcr.2008.04.003

Zheng, Y., Du, X., Wang, W., Boucher, M., Parimoo, S., & Stenn, K. (2005). Organogenesis from dissociated cells: generation of mature cycling hair follicles from skin-derived cells. *The journal of investigative dermatology*, *124*(5), 867–876. https://doi.org/10.1111/j.0022-202X.2005.23716.x

Zhu, N., Huang, K., Liu, Y., Zhang, H., Lin, E., Zeng, Y., Li, H., Xu, Y., Cai, B., Yuan, Y., Li, Y., & Lin, C. (2018). miR-195-5p Regulates Hair Follicle Inductivity of Dermal Papilla Cells by Suppressing Wnt/*β*-Catenin Activation. *BioMed research international*, *2018*, 4924356. https://doi.org/10.1155/2018/4924356

Zuk, P. A., Zhu, M., Ashjian, P., De Ugarte, D. A., Huang, J. I., Mizuno, H., Alfonso, Z. C., Fraser, J. K., Benhaim, P., & Hedrick, M. H. (2002). Human adipose tissue is a source of multipotent stem cells. *Molecular biology of the cell*, *13*(12), 4279–4295. https://doi.org/10.1091/mbc.e02-02-0105

.